

| | |
|---------------------|---|
| Zeitschrift: | Eclogae Geologicae Helvetiae |
| Herausgeber: | Schweizerische Geologische Gesellschaft |
| Band: | 99 (2006) |
| Heft: | 3 |
| Artikel: | Earthquake-induced deformation structures in lake deposits : a Late Pleistocene to Holocene paleoseismic record for Central Switzerland |
| Autor: | Monecke, Katrin / Anselmetti, Flavio S. / Becker, Arnfried |
| DOI: | https://doi.org/10.5169/seals-169245 |

Nutzungsbedingungen

Die ETH-Bibliothek ist die Anbieterin der digitalisierten Zeitschriften auf E-Periodica. Sie besitzt keine Urheberrechte an den Zeitschriften und ist nicht verantwortlich für deren Inhalte. Die Rechte liegen in der Regel bei den Herausgebern beziehungsweise den externen Rechteinhabern. Das Veröffentlichen von Bildern in Print- und Online-Publikationen sowie auf Social Media-Kanälen oder Webseiten ist nur mit vorheriger Genehmigung der Rechteinhaber erlaubt. [Mehr erfahren](#)

Conditions d'utilisation

L'ETH Library est le fournisseur des revues numérisées. Elle ne détient aucun droit d'auteur sur les revues et n'est pas responsable de leur contenu. En règle générale, les droits sont détenus par les éditeurs ou les détenteurs de droits externes. La reproduction d'images dans des publications imprimées ou en ligne ainsi que sur des canaux de médias sociaux ou des sites web n'est autorisée qu'avec l'accord préalable des détenteurs des droits. [En savoir plus](#)

Terms of use

The ETH Library is the provider of the digitised journals. It does not own any copyrights to the journals and is not responsible for their content. The rights usually lie with the publishers or the external rights holders. Publishing images in print and online publications, as well as on social media channels or websites, is only permitted with the prior consent of the rights holders. [Find out more](#)

Download PDF: 12.01.2026

ETH-Bibliothek Zürich, E-Periodica, <https://www.e-periodica.ch>

Earthquake-induced deformation structures in lake deposits: A Late Pleistocene to Holocene paleoseismic record for Central Switzerland

KATRIN MONECKE^{1,6}, FLAVIO S. ANSELMETTI², ARNFRIED BECKER³, MICHAEL SCHNELLMANN^{2,5},
MICHAEL STURM⁴ & DOMENICO GIARDINI¹

Key words: Paleoseismology, lake deposits, Central Switzerland, earthquake-induced sediment deformation, Late Pleistocene, Holocene

ZUSAMMENFASSUNG

In den bis zu 15.000 Jahre alten Sedimenten von vier Seen in der Zentralschweiz wurden Spuren von drei starken historischen und mindestens sieben prähistorischen Erdbeben gefunden. Der Schweizer Erdbebenkatalog der letzten 1000 Jahre verzeichnet in der Zentralschweiz drei grössere Erdbeben mit Magnituden zwischen $M_w=5.7$ und $M_w = 6.2$ (1964 AD Alpnach, 1774 AD Altdorf, 1601 AD Unterwalden) sowie ein katastrophales $M_w = 6.9$ Ereignis in Basel im Jahre 1356 AD. Zur Bestimmung der Wiederkehrraten dieser starken Erdbeben wurden mit Hilfe von hochauflösender Seismik und Sedimentkernanalysen paläoseismische Untersuchungen in vier verschiedenen Seen in der Zentralschweiz durchgeführt (Lungerer See, Baldegg See, Seelisberg Seeli und Vierwaldstätter See). In Abhängigkeit von der Geometrie des Seebeckens, des Sedimenttyps und der lokalen Bodenerschütterung treten während eines Erdbebens grosse subaquatische Rutschungen oder kleine in-situ Deformationsstrukturen auf. Die Spuren der historischen Erdbeben zeigen, dass Seesedimente nur ab einer Magnitude von $M_w>5.7$ und bei einer lokalen Bodenerschütterung der Intensität \geq VII deformiert werden. Mindestens sechs prähistorische Erdbeben in der Zentralschweiz (Epizentrum und Magnitude ähnlich wie beim $M_w=6.2$ Unterwalden Erdbeben), sowie ein starkes prähistorisches Erdbeben in der Baselregion (Magnitude ähnlich wie beim $M_w = 6.9$ Basel Erdbeben) konnten anhand der Art und regionalen Verteilung der Deformationsstrukturen bestimmt werden. Darüber hinaus gibt es Hinweise auf ein weiteres Ereignis in der Nähe von Basel und vier weitere Ereignisse in der Zentralschweiz. Im Vergleich zum Mittleren Holozän scheint die Erdbebenhäufigkeit in der Zentralschweiz erhöht während des Spätpleistozäns/Frühholozäns und während der letzten 4000 Jahre. Dies kann einerseits auf isostatische Ausgleichsbewegungen nach dem Abschmelzen des Eises vor 15.000 Jahren, sowie auf eine periodische Aktivierung einer alpinen seismogenen Zone in jüngerer Zeit zurückgeführt werden.

ABSTRACT

Traces of three larger historic and at least seven prehistoric earthquakes during the last 15,000 years were found in the sedimentary record of four lakes in Central Switzerland. The Swiss historic earthquake catalogue of approximately the last 1000 years reports three larger earthquakes in Central Switzerland with moment magnitudes varying between $M_w = 5.7$ and $M_w = 6.2$ (1964 AD Alpnach, 1774 AD Altdorf, 1601 AD Unterwalden) and the nearby catastrophic $M_w = 6.9$ event close to Basel in 1356 AD. In order to determine the recurrence intervals of such events and thus, the seismic hazard and risk, paleoseismic investigations were carried out in four different lakes of Central Switzerland (Lungerer See, Baldegg See, Seelisberg Seeli, Vierwaldstätter See) using high-resolution seismic data and sediment core analyses. Depending on lake basin geometry, sediment type and local ground shaking earthquake-induced deformation structures comprise large-scale mass movement deposits and small-scale in-situ deformation features. The signatures of historic earthquakes show that lacustrine sediments are only affected by seismic shocks of a minimum magnitude of $\sim M_w = 5.7$ and within or close to the isoseismal line of intensity VII. Traces of at least six prehistoric events in Central Switzerland of similar size and magnitude than the $M_w = 6.2$ 1601AD Unterwalden earthquake and one prehistoric 1356AD Basel-type earthquake are determined by evaluating the type of deformation and the basin-wide as well as the regional distribution of deformations. One further event in the Basel region and four events in Central Switzerland are less well defined in the sedimentary record. Compared to the Mid Holocene earthquake frequency in Central Switzerland seems to be enhanced during Late Pleistocene/Early Holocene time and during the last 4000 cal y BP, which can be related to isostatic rebound after the ice retreat starting at about 15,000 cal y BP and a periodic activation of a seismogenic zone in the Alps during recent times.

Introduction

The Swiss historic earthquake record covering approximately the last 1000 years shows an enhanced seismicity in Central Switzerland (Fäh et al. 2003; Deichmann et al. 2000). This includes three major earthquakes in 1964 AD, 1774 AD and

1601 AD with moment magnitudes of $M_w = 5.7$, 5.9 and 6.2, respectively (uncertainties on historic earthquakes are estimated at ± 0.5 magnitude units and ± 0.5 to 1.0 intensity units, European Macroseismic Scale, EMS). They occurred within the today densely populated areas of Sarnen, Altdorf and Un-

Corresponding author: Katrin Monecke. E-mail: kmonecke_gst@kent.edu

¹Geophysical Institute, ETH Hönggerberg, 8093 Zürich, Switzerland

²Geological Institute, ETH Zürich, Sonneggstr. 5, 8092 Zürich, Switzerland

³Sonneggstr. 57, CH-8006 Zürich, Switzerland

⁴Sedimentology Section/Department of Surface Waters (SURF), EAWAG, 8600 Dübendorf, Switzerland

⁵Nagra, Hardstr. 73, CH-5430 Wettingen, Switzerland

⁶Department of Geology, Kent State University, 212 McGilvrey, Kent, OH 44242, USA

terwalden and caused life-tolls and severe building damages. Furthermore, the northern part of Central Switzerland was affected by the catastrophic 1356AD Basel event with a magnitude of $M_w = 6.9$ (Fäh et al., 2003; Mayer-Rosa & Cadiot, 1979).

Central Switzerland is situated within the Alpine range showing nowadays a low deformation rate and a long seismic cycle. According to the 1000-year-long historic earthquake catalogue, the 1601 AD Lucerne earthquake as well as the 1356 AD Basel earthquake are unique events within the specific region, indicating that recurrence intervals are up to several hundreds of years, which is beyond the dataset of the historic earthquake catalogue. Therefore, geological archives have to be investigated in order to determine the frequency and size of large events and thus, the regional seismic hazard.

The most common paleoseismic method is the “on-fault” mapping of surface deformations that are caused by movement of an active fault. It allows the direct measurement of displacement rates along the fault and the determination of the earthquake size. So-called “off-fault” seismic evidences include earthquake-induced mass movements (e.g. Jibson, 1996) and soft sediment deformation features like liquefaction structures (e.g. Obermeier, 1996; Galli & Ferrel, 1995). Paleoseismic studies are often carried out within subaerial alluvial settings, which represent a highly dynamic sedimentary environment, that may render the identification of earthquake-induced deformations difficult. Furthermore, the occurrence of strong erosion can lead to an incomplete paleoseismic record. Lake deposits, on the other hand, generally form a quiet, highly sensitive and complete sedimentary archive (Ricci Lucchi, 1995). Earthquake-induced deformations in lake sediments comprise large-scale mass movements as well as small-scale in-situ deformation structures. Paleoseismic studies have been successfully carried out in outcrops of lacustrine sediments (for example Sims 1973 and 1975; Marco et al. 1996; Ringrose 1989; Rodriguez-Pascua et al. 2000; Hibscher et al. 1997). In modern lakes, investigations are based on high-resolution seismic data (Shilts & Clague 1992; Chapron et al. 1999) and more rarely on sediment cores (Doig 1986; Becker et al. 2002, Migowski et al. 2004).

Paleoseismic studies in Central Switzerland started in Vierwaldstätter See (Lake Lucerne): Siegenthaler et al. (1987) and Siegenthaler & Sturm (1991) observed mega-turbidites caused by mass failure during the historical 1601 AD and 1774 AD earthquakes. Furthermore, the youngest sediments of four smaller lakes around Vierwaldstätter See were investigated for traces of historically reported earthquakes to calibrate earthquake-induced deformation in lake sediments (Monecke et al. 2004). Based on a detailed seismic survey in Vierwaldstätter See, Schnellmann et al. (2002) proposed four larger, prehistoric earthquakes in Central Switzerland during the Late Pleistocene/Holocene indicated by multiple contemporaneous mass failure at different lake sides. In order to complete this paleoseismic record and to determine, if possible, epicenter and magnitude of prehistoric events, the present study focuses on

three smaller lakes around Vierwaldstätter See distributed within an area of approximately 2000 km²: Lungerer See, Baldegger See and Seelisberg Seeli. The lakes were studied using high-resolution seismic data and sediment cores. Deformation structures clearly distinguishable from the regular lake sedimentation and potentially generated during seismic shocks are described and dated. A probability of earthquake-triggering is assigned to these so-called events depending on the distribution of deformation throughout the single lake basins, and on type and intensity of deformation. In a second step, events are correlated between the different lakes including paleoseismic data from Vierwaldstätter See as well as from the Basel region. Considering the type and regional distribution of deformations, possible prehistoric earthquakes in Central Switzerland are determined.

Geological and seismotectonic setting

The investigated lakes are located in Central Switzerland close to the northern border of the Alpine range, where the Helvetic nappes are thrust over the Molasse basin. In this region several overdeepened basins were formed by glacier erosion during the last glaciations. After the progressive retreat of ice after the Last Glacial Maximum starting at about 15,000 y BP, several lakes formed and continuous lacustrine sedimentation started.

Although the instrumentally recorded seismicity in Central Switzerland during the last 30 years is extremely low, the historic earthquake catalogue indicates several damaging earthquakes during the last 500 years (Fig. 1; Deichmann et al. 2000; Fäh et al. 2003). The largest known events are the 1601 AD Unterwalden, 1774 AD Altdorf and the 1964 AD Sarnen earthquakes with moment magnitudes of $M_w = 6.2$, $M_w = 5.9$ and $M_w = 5.7$, respectively. The epicenters are located within the Helvetic domain and are concentrated around Sarnen and Altdorf (Fig. 1b). Characteristic is the occurrence of earthquake swarms including one or more larger events: During the most recent 1964 AD Sarnen earthquake with a magnitude of $M_w = 5.7$, for example, more than 1000 events were recorded, including a $M_w = 5$ event only one month before the main shock. Focal depths are remarkably low and lie in a few kilometers depth within the Helvetic nappes (Deichmann et al., 2000). Only a few focal mechanisms could be determined which point to WNW-ESE and NNE-SSW striking fault planes. Remarkably is that normal and reverse faulting occur very close to each other, which indicates either a very heterogeneous stress field or a small difference between the smallest and largest stress (Deichmann et al. 2000).

The Basel region belongs to the Cenozoic rift system of the Upper Rhine Graben. The instrumentally measured recent seismicity since 1975 has been relatively weak, while the pre-instrumental macroseismic earthquake catalogue shows that the Basel region was affected by at least 3 to 4 larger earthquakes with magnitudes of $M_w \geq 5$ during the last 1000 years. This includes the October 18, 1356 earthquake of Basel,

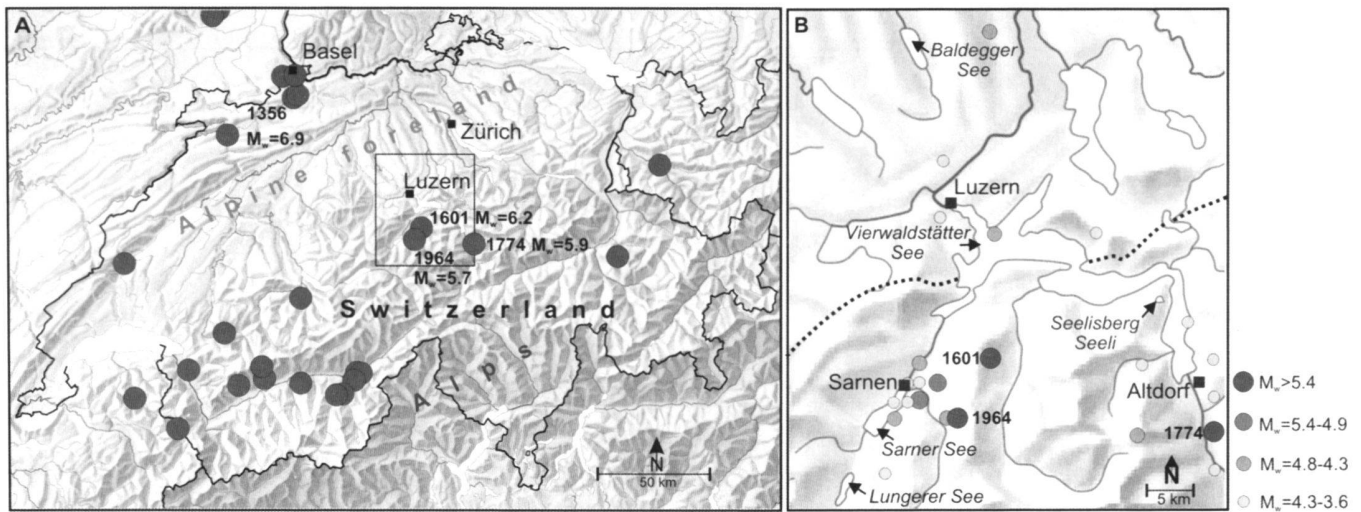


Fig. 1. A) Historic seismicity in Switzerland and surrounding areas. B) Location of studied lakes. Dashed line marks northern Alpine front. Dots mark epicenters of historic earthquakes of the last 1000 years with moment magnitudes $M_w > 3.6$ (Fig. 1A) and $M_w > 5.4$ (Fig. 1B; after Fäh et al., 2003).

which is the largest known earthquake in northern central Europe with $M_w = 6.9$. Investigations of recent earthquakes in the Basel region indicate relatively shallow hypocentral depths located mostly between 5 km and 15 km below the surface (Deichmann et al., 2000). Calculated focal mechanisms of some larger earthquakes show a predominance of strike-slip faults and normal faults with ENE-WSW direction of extension.

Methods

A dense grid of high-resolution seismic lines was obtained in each of the investigated lakes using a 3.5 kHz pinger source. Navigation was optimized to a precision of ± 2 meters using differential GPS.

The data was processed using the SPWTM seismic processing software package. The raw data was muted, bandpass filtered (1500–6500 Hz) and gained with the “Automatic gain control” – function. The seismic lines were interpreted using 2D KingdomSuiteTM interpretation software. Water and sediment depth were calculated assuming a velocity of 1500 ms⁻¹.

Short cores with a diameter of 5.8 cm and a length up to 2 m were taken with a gravity corer. Several long sediment cores with the same diameter were taken from coring platforms using two different piston coring systems: In Baldegger See and Lungerer See Kullenberg piston cores up to a length of 8 m were taken as entire pieces (for description of the coring system see Kelts et al. 1986). In a second coring campaign in Lungerer See, as well as in Seelisberg Seeli, UWITEC piston cores were taken. This coring system penetrates also through coarser-grained and very stiff sediment, so that deeper stratigraphic levels up to a sediment depth of ~20 m can be reached. As the 3 m long coring barrel can be kept closed, cor-

ing can start at some depth below the lake bottom, where the piston is released from the barrel tip. The sedimentary record is recovered in a stepwise coring of 3 m long pieces with an overlap of 50 cm to 100 cm.

The cores were cut in ~1 m long sections and stored in a cold room at 4° C. Before opening the cores were scanned using a GEOTEK Ltd. multi sensor core logger in order to obtain petrophysical data (p-wave velocity, gamma ray density and magnetic susceptibility).

Cores were split into two halves and photographed immediately after opening, followed by sedimentological description. Characteristic units were sampled (smear slides, sampling for radiocarbon dating) and photographed in detail.

Preparation and pre-treatment of sample material for radiocarbon dating was carried out by the ¹⁴C laboratory of the Department of Geography at the University of Zurich (GIUZ). The dating itself was done using the accelerator mass spectrometry (AMS) with the tandem accelerator of the Institute of Particle Physics at the Swiss Federal Institute of Technology Zurich (ETH) and the Paul Scherrer Institute (PSI). Radiocarbon ages were calibrated using the calibration program OxCal v. 3.8 (Bronk Ramsey, 1995, 2001; Stuiver et al. 1998).

Dating of lake sediments

The dating and correlation of deformation structures throughout a single lake basin and between the different lakes is crucial for the interpretation of a regional and potentially paleoseismic event (McCalpin 1996, Davenport 1994). The uppermost sedimentary record of the last approximately 500 years can be quite accurately dated by using historic data about climate and environmental changes, flood events, spontaneous

Table 1. Results of radiocarbon dating of sediments from Lungerer See, Seelisberg Seeli and Baldegger See. Calibration according to calibration program OxCal v. 3.8 (Bronk Ramsey 1995 and 2001).

| Lake | Sample | Depth (cm) | Lab code | Conventional radiocarbon age (BP) | 2 sigma range of calibrated radiocarbon age (BP) | Mean value of 2 sigma range (BP) | δ13C (‰) | Material |
|------------------|-----------------|------------|----------|-----------------------------------|--|----------------------------------|----------|---------------|
| Lungerer See | Lng00-1_2_60 | 170 | UZ-4698 | 555±50 | 650-510 | 580 | -22,9 | leaves |
| | Lng00-1_2_61 | 171 | UZ-4938 | 230±60 | 460-(1960AD) | 225 | -23,6 | leaves |
| | Lng00-1_4_69 | 380 | UZ-4939 | 2830±55 | 3140-2780 | 2960 | -22,4 | leaves |
| | Lng00-1_5_97 | 510 | UZ-4940 | 415±50 | 540-310 | 425 | -20,8 | leaves |
| | Lng00-1_6_68 | 580 | UZ-4699 | 365±45 | 510-310 | 410 | -23,9 | leaves (?) |
| | Lng00-1_6_97 | 610 | UZ-4641 | 510±50 | 600-470 | 535 | -20,9 | leaves |
| | Lng02-2_AIII_64 | 660 | UZ-5063 | 1155±60 | 1240-930 | 1085 | -24,8 | plant remains |
| | Lng02-2_BI_90 | 730 | UZ-5064 | 1315±80 | 1370-1050 | 1210 | -22,9 | plant remains |
| | Lng02-3_AII_48 | 870 | UZ-5065 | 1575±50 | 1570-1340 | 1455 | -23,9 | leaves |
| | Lng02-2_BII_87 | 875 | UZ-5066 | 1750±65 | 1830-1520 | 1675 | -17 | plant remains |
| | Lng02-3_AIV_36 | 920 | UZ-5074 | 2385±50 | 2720-2330 | 2525 | -21,2 | leaves |
| | Lng02-1_1CII_29 | 990 | UZ-5073 | 1330±50 | 1350-1140 | 1245 | -25,3 | leaves |
| | Lng02-1_CIII_27 | 1080 | UZ-5067 | 1575±50 | 1570-1340 | 1455 | -24 | leaves |
| | Lng02-3_BII_76 | 1150 | UZ-5068 | 2705±50 | 2930-2740 | 2835 | -24,5 | leaves |
| | Lng00-4_5_19 | 420 | UZ-5070 | 460±45 | 560-330 | 445 | -21,8 | leaves |
| Baldegger See | Lng00-4_6_7 | 500 | UZ-5071 | 1975±55 | 2110-1810 | 1960 | -21,8 | leaves |
| | Lng00-4_7_16 | 600 | UZ-5072 | 2370±65 | 2750-2150 | 2450 | -18,9 | leaves |
| | Lng00-6_4_3 | 250 | UZ-4937 | 2055±55 | 1890-2150 | 2020 | -22,3 | leaves |
| | Lng00-6_4_52 | 300 | UZ-4700 | 1710±55 | 1820-1420 | 1620 | -22,9 | leaves |
| | Ba02-7b_46 | 50 | UZ-4905 | 335±55 | 510-290 | 400 | -22,9 | leaves |
| | Ba02-7b_58 | 70 | UZ-4904 | 300±45 | 480-280 | 380 | -22,9 | plant remains |
| | Ba02-4b_79 | 120 | UZ-4902 | 670±50 | 690-540 | 615 | -20,3 | leaves |
| | Ba02-4b_97 | 155 | UZ-4903 | 785±45 | 790-650 | 720 | -30,2 | plant remains |
| | Ba97-3_4_78 | 265 | UZ-4690 | 1625±55 | 1700-1380 | 1540 | -22,3 | leaves (?) |
| | Ba97-3_5_33 | 310 | UZ-4691 | 1850±65 | 1930-1600 | 1765 | -23,7 | leaves (?) |
| | Ba97-3_6_17 | 385 | UZ-4729 | 2800±50 | 3080-2770 | 2925 | -29 | leaves |
| | Ba97-3_6_83 | 450 | UZ-4692 | 3330±55 | 3700-3440 | 3570 | -23,2 | leaves (?) |
| | Ba97-3_7_3 | 465 | UZ-4693 | 3630±70 | 4150-3720 | 3935 | -22,1 | leaves (?) |
| | Ba97-3_7_19 | 480 | UZ-4694 | 3695±75 | 4250-3830 | 4040 | -21,9 | leaves (?) |
| | Ba97-3_7_73 | 530 | UZ-4695 | 4550±65 | 5460-4970 | 5215 | -23,6 | leaves (?) |
| | Ba00-4_4_29 | 560 | UZ-4697 | 5350±65 | 6290-5950 | 6120 | -21,7 | leaves (?) |
| | Ba97-3_8_49 | 600 | UZ-4730 | 6335±85 | 7430-7010 | 7220 | -21,8 | leaves |
| | Ba97-3_9_23 | 660 | UZ-4696 | 7725±70 | 8640-8380 | 8510 | -24,8 | leaves (?) |
| | Ba97-3_9_58 | 700 | UZ-4731 | 7995±80 | 9150-8550 | 8850 | -31,9 | leaves (?) |
| Seelisberg Seeli | Sel01-3_I | 90 | UZ-4649 | 365±50 | 510-310 | 410 | -17,3 | leaves |
| | Sel01-5_AII_77 | 160 | UZ-4935 | 555±55 | 650-500 | 575 | -22,2 | leaves |
| | Sel01-5_AIII_90 | 295 | UZ-4809 | 1545±50 | 1540-1320 | 1430 | -25,5 | leaves |
| | Sel01_6_BIII_85 | 330 | UZ-4735 | 2265±50 | 2360-2150 | 2255 | -21,7 | leaves (?) |
| | Sel01_6_CII_5 | 425 | UZ-4804 | 2525±65 | 2760-2360 | 2560 | -24,3 | leaves |
| | Sel01-5_BIII_16 | 480 | UZ-4800 | 2920±70 | 3320-2870 | 3095 | -23,3 | plant remains |
| | Sel01-6_CIII_90 | 555 | UZ-4805 | 3780±55 | 4360-3980 | 4170 | -20,4 | leaves |
| | Sel01-6_DII_11 | 620 | UZ-4734 | 5920±75 | 6940-6540 | 6740 | -23,3 | plant remains |
| | Sel01-6_DII_96 | 680 | UZ-4806 | 5400±60 | 6300-5990 | 6145 | -25,1 | plant remains |
| | Sel01-6_DIII_84 | 720 | UZ-4807 | 6875±65 | 7840-7580 | 7710 | -23 | plant remains |
| | Sel01-6_EII_8 | 740 | UZ-4808 | 6695±65 | 7670-7430 | 7550 | -22,6 | leaves (?) |
| | Sel01-6_EIII_29 | 825 | UZ-4812 | 9765±80 | 11350-10750 | 11050 | -26,8 | leaves |
| | Sel01-6_DIII_44 | 830 | UZ-4811 | 10065±80 | 12150-11200 | 11675 | -21,6 | plant remains |
| | Sel01-6_FI_61 | 850 | UZ-4813 | 10805±80 | 13130-12630 | 12880 | -19,2 | leaves (?) |

mass movements and artificial lake level regulations. Varves were counted in certain intervals, giving an idea about annual sedimentation rates. Well-dated ash layers of the Laacher See and probably also the Vasset/Killian volcanic eruptions (Hajdas et al. 1993) were found in the deeper sedimentary record of Baldegger See. In addition to this sedimentological data, about 50 radiocarbon ages were obtained in the three investigated lakes (Table 1). Ideal radiocarbon samples are terrestrial leaves within regular deposited lake sediments. It has to be considered that radiocarbon ages tend to be too old because of dating of old and reworked material and therefore, represent maximum ages. Furthermore, 2-sigma age ranges of calibrated radiocarbon ages vary between 130 and 950 years. Within this study we propose for Lungerer See, Baldegger See and Seelis-

berg Seeli a depth/age relationship based on the historic data and calibrated radiocarbon ages including the uncertainty ranges. Large-scale mass movement deposits are considered as instantaneous events and are not considered in the calculation of sedimentation rates. Some samples, which appear too old and deviate from the general trend of one curve are excluded from the age model. The deformation structures are dated by correlating the top of deformed strata to the corresponding age range.

Earthquake-induced deformation structures in lake sediments

Off-fault coseismic deformation structures in lacustrine sediments comprise large-scale mass movements and small-scale

in-situ deformation structures. Sub-aqueous mass failure takes place at the lake sides and can involve different processes of sliding, slumping and flowing of near-shore lake sediments. If the lake is bordered by steep cliff faces within high-relief mountain areas, rockfalls may occur during earthquake shaking. Mobilized masses may cause deformation within the underlying and frontal lake sediments forming “fold-and-thrust belt structures” (Schnellmann et al. 2005). The mass movement deposits are not only found close to the steep lake sides but might have been spread far into the central, flat-lying lake basins. During sub-aqueous mass failure generally a large quantity of fine-grained material is brought into suspension. It settles down in the deepest part of the basin forming a thick, nearly homogeneous turbidite sometimes with a coarser-grained base (“homogenite”, Sturm et al. 1995; Chapron et al. 1999). This turbidite might show slight periodically changing grain-size variations indicating an oscillating, standing wave (seiche) triggered by earthquake shaking or water displacement during mass-failure.

Mass movements in lakes occur not only during seismic shaking. Large lake level variations or strong wave action can cause liquefaction and mass-failure. Sediment overloading at oversteepened slopes leads to spontaneous slope instabilities and massive delta collapses. Therefore, a single mass movement deposit cannot clearly be interpreted as coseismic deformation feature. Only if multiple mass failure occurs contemporaneously at different lake sides a regional trigger mechanism like an earthquake is highly probable, requiring the correlation of several mass movement deposits throughout the entire lake basin (Schnellmann et al. 2002).

Small-scale in-situ deformation structures occurring within distinct horizons can often be identified as true earthquake-induced structures, so-called seismites (Seilacher 1969). Earthquake-induced faulting has been observed by several authors (Seilacher et al. 1969; Ringrose 1989; Becker et al. 2002). It occurs within more consolidated lake sediments stiff enough to show brittle failure, such as buried sediments in a few dm depth, fast consolidating carbonate-rich mud or jelly-like gyttja (e.g. Becker et al. 2002). Soft-sediment deformations like load casts and pseudonodules are generated by cyclic loading during earthquake shaking and subsequent liquefaction and reorganization of a gravitational unstable succession of layered lake sediments (Allen, 1982; Anketell, 1970). Liquefaction of sandy to silty layers causes sanddykes and mushroom-like intrusions into overlying sediments (Rodriguez-Pascua et al. 2000). Folded layers indicate ductile deformation during horizontally applied shear stress of seismic waves. Finely laminated sequences like varves can be disturbed during seismic shocks forming so-called “mixed layers” during stronger events of sufficient duration and amplitude (Rodriguez-Pascua et al. 2000; Marco et al. 1996; Migowski et al. 2004).

In-situ deformation structures can also be of non-seismic origin, so that other trigger mechanisms have to be excluded for paleoseismic studies. During deposition of large-scale slides and slumps, for instance, underlying lake sediments can be de-

Lungerer See

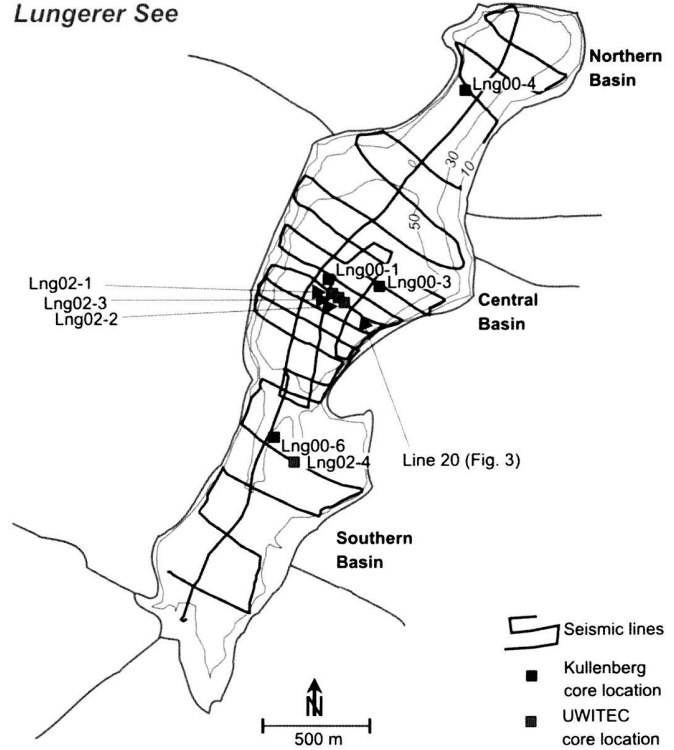


Fig. 2. Bathymetry, seismic survey grid and coring locations of Lungerer See.

formed (Schnellmann et al. 2005). High sedimentation rates and rapid, massive sediment load causes synsedimentary faults and liquefaction structures. Large lake level oscillations or strong wave action can generate liquefaction structures (Allen 1987). Furthermore, bioturbation can disturb the layered lake sediments. Finely laminated sediments, which are ideally varves, that indicate a quiet sedimentary environment with low sedimentation rates seem to be most favourable for the identification of earthquake-induced deformation (Rodriguez-Pascua et al. 2000, Marco et al. 1996).

Small-scale in-situ deformation structures are sometimes difficult to be recognized in sediment cores because of the limited available exposure of only a few centimeters. They can also largely vary throughout the lake basin and differ from core to core (Monecke 2004). The sediment cores that are like a pinprick may just miss deformation structures such as a sanddyke. Furthermore, it has to be considered that the sediment can be deformed during the coring procedure (Lotter et al. 1997b). Therefore, it is necessary to investigate two or more cores from one lake basin in order to correlate deformation structures throughout the lake basin and to determine a seismic event.

In the following chapters we describe so-called “events” for the sedimentary records of Lungerer See, Baldegger See and Seelisberg Seeli, which are marked by deformation structures that are potentially generated during earthquakes.

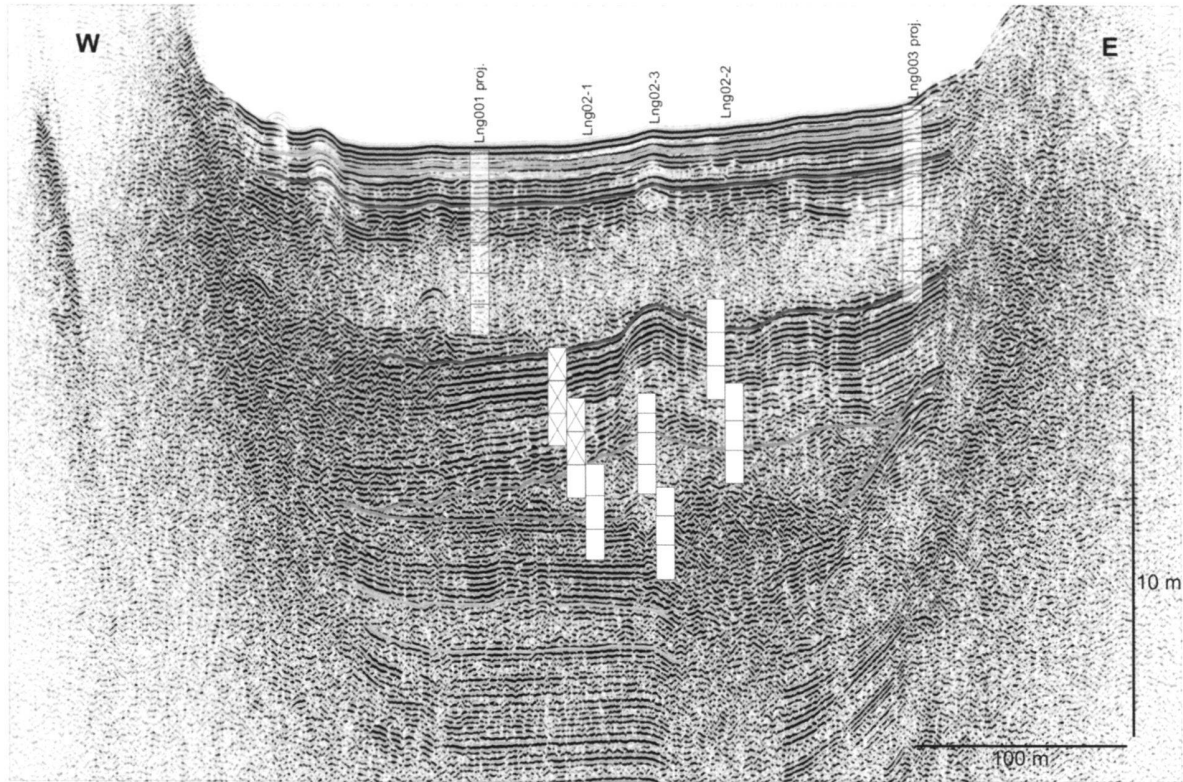


Fig. 3. High resolution seismic cross profile (line 20) through the central basin of Lungerer See. Events comprising units of chaotic seismic facies, which are interpreted as large-scale mass movement deposits, are marked in color. Sediment cores, indicated with individual sections, penetrate through the yellow, blue and green units but do not reach the pink one. For coring locations and position of seismic line see Fig. 2.

Deformation structures in Lungerer See

Lungerer See has a surface area of $\sim 3 \text{ km}^2$ and lies within a NNE-SSW striking Alpine valley at an altitude of 689 m a.s.l. (Fig. 1b). The lake is divided by subaqueous hardrock swells into three different sub-basins reaching a maximum water depth of 68 m in the central basin (Fig. 2). There are several inflows including a major tributary at the southern end building up a large delta in this basin.

A dense grid of seismic lines was obtained for Lungerer See (Fig. 2). The seismic lines show generally a good penetration of the acoustic signal down to a maximum sub-lake floor depth of 30 m, but partly the seismic penetration can be lower probably because of gas-rich sediments. The best subsurface information was obtained in the central basin where seismic lines display mainly continuous horizontally-layered seismic facies representing the regular lake sedimentation (Fig. 3). Large-scale units of chaotic seismic facies with irregular shape and thicknesses up to 7.5 m occur. These are interpreted as mass movement deposits interrupting the regular sedimentation (Schnellmann et al. 2002; Chapron et al. 1999) and are named with four colors from the youngest to the oldest: yellow, blue, green and pink. Correlation of the uppermost yellow and blue units to the northern and southern basin is possible,

whereas interbasinal correlation for the deeper events is uncertain.

Four Kullenberg and three UWITEC cores were taken in Lungerer See with an overlap between the different cores (Fig. 2, Fig. 3). The sediment cores in the central basin reach a maximum sediment depth of 12 m and penetrate through the yellow, blue and green units, but do not reach the pink one. The most complete sedimentary record of Lungerer See was obtained in the central basin showing clastic-dominated sedimentation (Fig. 4). Regularly deposited sediment consists of diffusely layered light- to dark-gray silty clays reflecting seasonally changing fluvial input. A large number of sandy to clayey graded turbidites, which are a few mm up to 20 cm thick, occur throughout the sedimentary record and were probably generated during flood events. The large-scale mass movement deposits, which can be seen also in the seismic data, consist of massive silty clays and overthrust units of layered lake sediments and are often overlain by thick slump-generated turbidites. A depth/age relationship is proposed for the sedimentary record in the central basin of Lungerer See reaching back to $\sim 1500 \text{ y BP}$ and indicating rather high sedimentation rates of 40 cm in 100 years (Fig. 4). The lowermost obtained radiocarbon ages in the central (Fig. 4) as well as in the northern basin (Fig. 5) are between 2000 and 3000 cal y

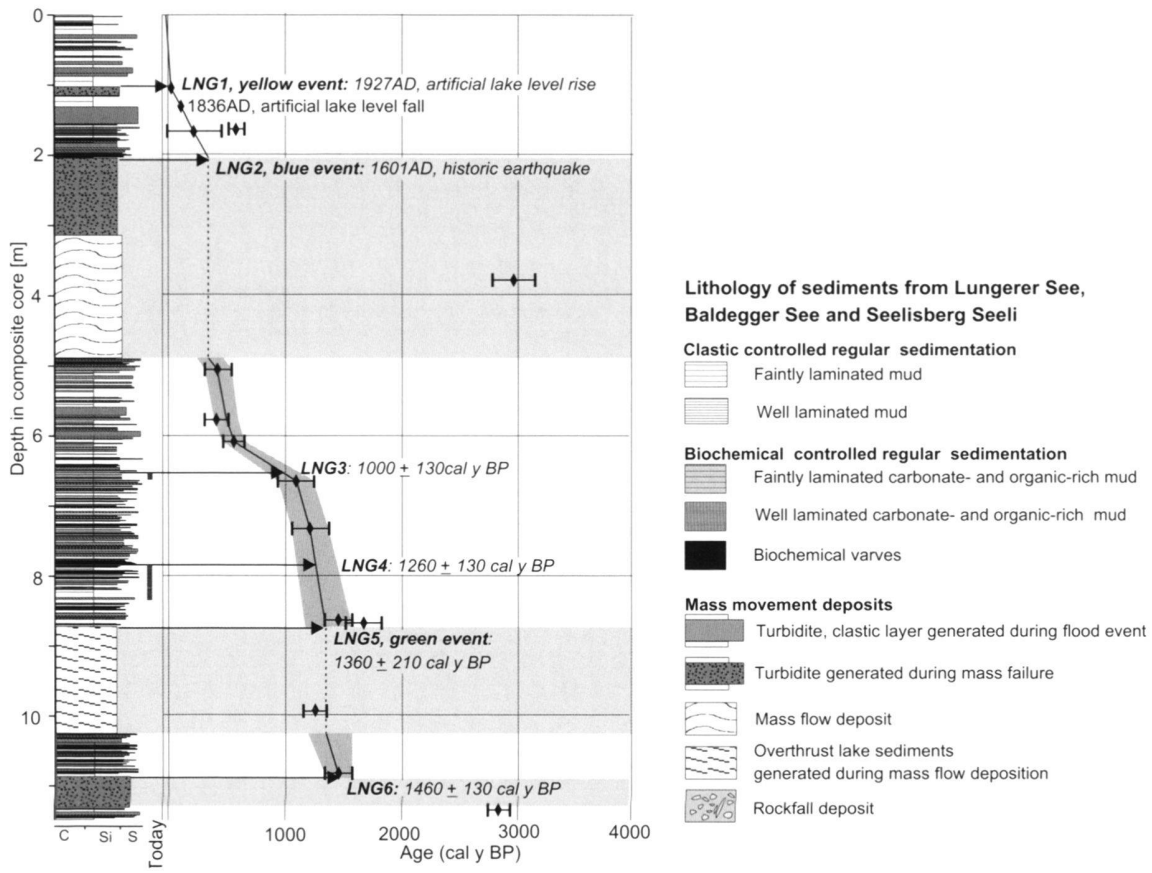


Fig. 4. Composite lithology log and depth/age relationship of sediments in the central basin of Lungerer See. Radiocarbon ages are mean values of calibrated 2 sigma age ranges (cal y BP, see table 1). Artificial lake level variations after Ming (1991). Correlation of historic earthquakes after Monecke et al. (2004). Vertical bars at lithology log small-scale deformation structures. Arrows mark top of deformed units correlating with the age of events.

BP indicating that older sediments were recovered at the base of the cores.

Figure 5 summarizes the seismic-to-core and core-to-core correlations, which are based on the tracing of the four seismic stratigraphic event horizons (yellow, blue, green and pink) and several marker turbidites named T1 to T56 that can be followed throughout sub-basins. Deformation structures of Lungerer See are related to seven events, named LNG1-LNG7 including the four events, which can be seen in the seismic data. They mark exclusively mass movement deposits of different size and from varying sediment sources:

LNG1, yellow event: The most recent event occurs in ~1 m depth of the sedimentary record and comprises small-scale mass flow deposits at the lake sides grading into coarse-grained turbidites towards the central basin (Fig. 3, Fig. 5). In the southern basin an erosional surface is seismically visible in the same depth. The yellow event corresponds to the artificial lake level lowering of nearly 40 m in 1836 AD followed by the redamming of the lake in 1927 AD (Ming 1991; Monecke et al. 2004). Erosion occurred in the drained southern basin during lake level lowstand after 1836 AD. After re-damming of the

lake intensive reworking of the shore deposits took place, causing mobilization of near-shore lake deposits.

LNG2, blue event: The blue event occurs in a sediment depth of 2 m in the central basin and comprises huge mass movement deposits reaching a maximum thickness of 7.5 m (Fig. 3, Fig. 5). The top is formed by an up to 1 m thick homogenite. The thickness distribution derived from the seismic data, shows three different depositional centers in the central and northern basin indicating multiple mass failure. In the southern basin a hiatus occurs within the sedimentary record (Fig. 5), which can be explained by a large delta collapse during basin-wide mass-failure. The blue event is correlated to the historic Unterwalden earthquake in 1601 AD (Monecke et al. 2004).

LNG3 and LNG4: Between marker turbidites T30 and T31 and between T11 and T15 two smaller mass movement deposits can be found in the sediment cores in the eastern part of the central basin (Fig. 5). These small-scale units are probably generated due to slope instabilities within the nearby delta deposits at the eastern lake side of the central basin (Fig. 2). Mass-failure took place at ~1000 cal y BP and ~1260 cal y BP (Fig. 4).

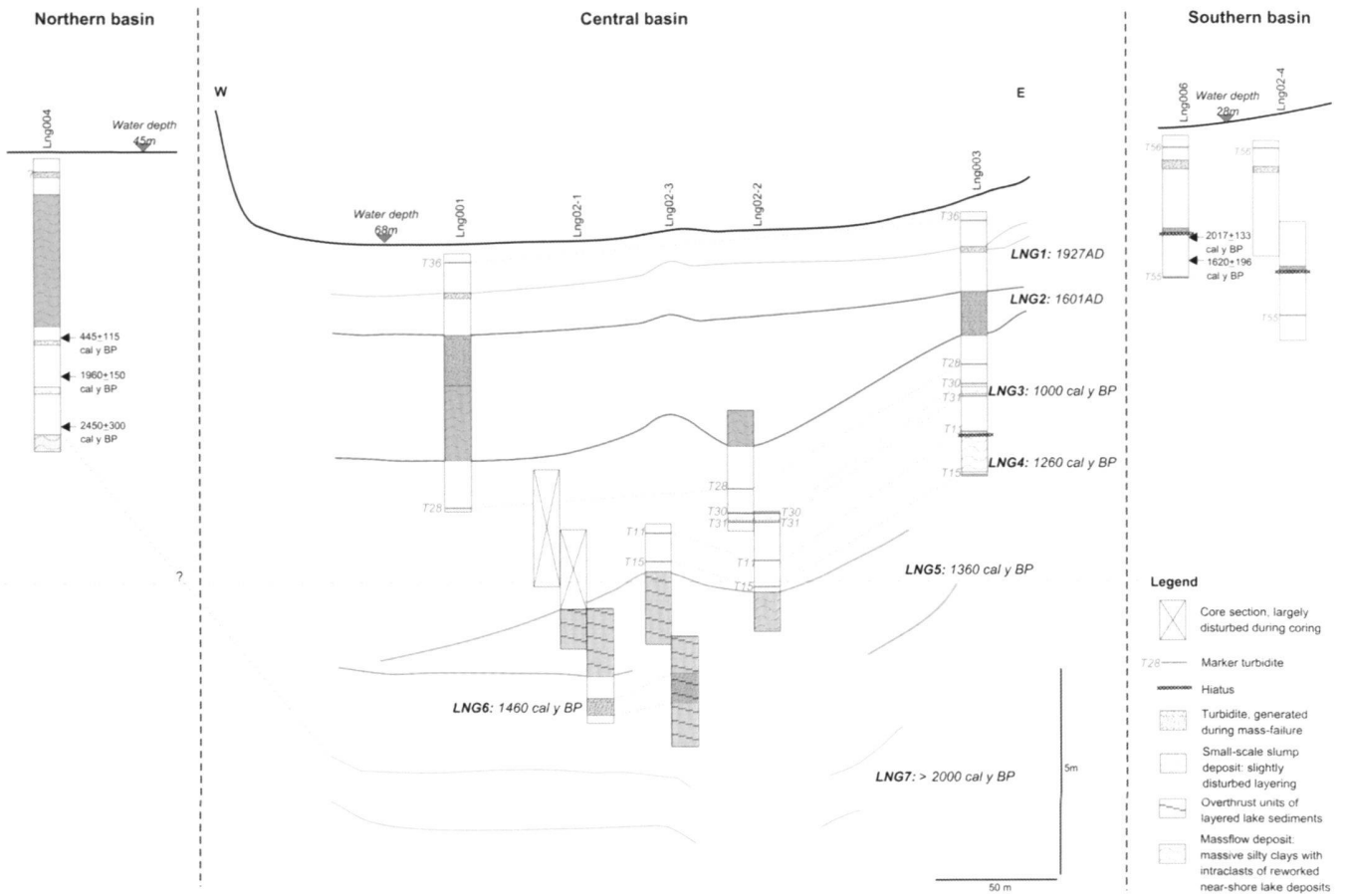


Fig. 5. Seismic-to-core and core-to-core correlations of events and marker turbidites within the sedimentary record of Lungerer See.

LNG5, green event: A larger mass movement deposit occurs in a sediment depth of about 8.5 m in the central basin comprising a massflow unit in the eastern part grading laterally into stacked and multiple overthrust segments of layered lake sediments in the western part (Fig. 3, Fig. 5). Remarkable is the build-up of a “bump” in the middle of the central basin and the lack of a massflow-generated turbidite. The maximum thickness reaches 2.5 m and decreases from the East towards the West indicating transport from delta deposits in the Eastern part of the central basin, with the massflow largely deforming the underlying sediments. The deposition of the green unit occurred around 1360 cal y BP (Fig. 4).

LNG6: Event LNG6 in a depth of ~11 m in the central basin comprises a 45–70 cm thick mega-turbidite/“homogenite”, which became partly incorporated into the overthrust lake sediments of the green unit (Fig. 5). The turbidite was probably generated during mass failure, however, the related moving mass was not reached with the sediment cores. It likely can be found right below the green unit in the Eastern part of the central basin, though it cannot clearly be distinguished in the seismic data (Fig. 3). The event LNG6 has an age of ~1450 cal y BP (Fig. 4).

LNG7, pink event: At a sediment depth of ~13 m the seismic lines of the central basin image an additional large-scale mass movement deposit reaching a maximum thickness of 2 m (Fig. 3, Fig. 5). It probably correlates with an up to 3 m thick mass movement deposit in the northern basin, which can be seen in the seismic data and is reached at the base of core LNG004 (Fig. 5). The thickness distribution of the pink unit indicates four depositional centers characteristic for multiple slumping within different delta deposits in the central and southern basin and at the northern lake side (Fig. 6). Assuming similar sedimentation rates like in overlying sediments (40 cm in 100 years) a minimum age of about 2000 cal y BP can be assigned to the pink event (Fig. 4). Considering the lowermost obtained radiocarbon ages above the pink unit of 2835 +/- 95 cal y BP in the central and 2450 +/- 300 cal y BP in the northern basin, this event can be even older.

Deformation structures in Baldegger See

Baldegger See is located in the northern Alpine foreland at an altitude of 463 m a.s.l. (Fig. 1b). It has a maximum water depth of 66 m and a surface area of 5.2 km² (Fig. 7). There are sever-

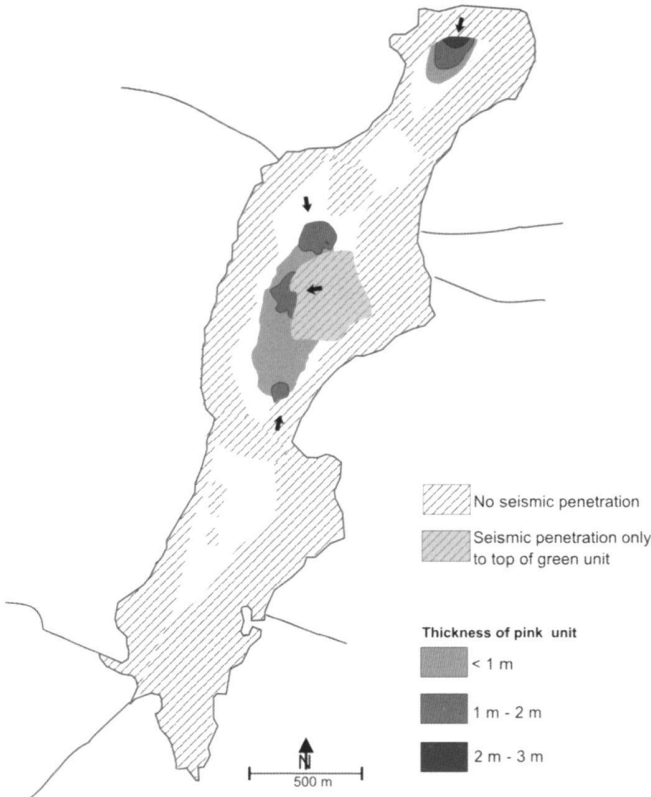


Fig. 6. Thickness distribution of the pink unit in Lungerer See indicating four different depositional centers and transport directions.

al small tributaries feeding the lake including a major one at the southern end. The seismic lines show only locally a good penetration of the acoustic signal probably because of gas-rich sediments. Therefore, the paleoseismic investigations are mainly based on 7 short and 4 long sediment cores taken in the deepest, central part of the basin (Fig. 7).

Sedimentation in Baldegg See is dominated by biochemical processes within the lake (Fig. 8, Fig. 9). The regularly deposited sediment consists mainly of faintly to well-laminated carbonate-rich mud. Remarkable are several up to 70 cm thick intervals of finely-laminated mud with alternating black, organic-rich and white, calcite-rich laminae. They are interpreted as biochemical varves forming under warmer and/or nutrient-rich conditions (Lotter et al. 1997a). The varves are best preserved within cores taken in the deepest part of the basin, whereas towards shallower water they become thinner and more disturbed. Some coarser-grained, only a few centimeter thick clastic layers and turbidites, which were probably generated during flood events, occur throughout the sedimentary record.

The recovered sedimentary record reaches back to about 16,000 cal y BP (Fig. 8). Overall sedimentation rates are rather low varying between 10–15 cm in 100 years. The depth/age relationship shows an increased sedimentation rate towards the

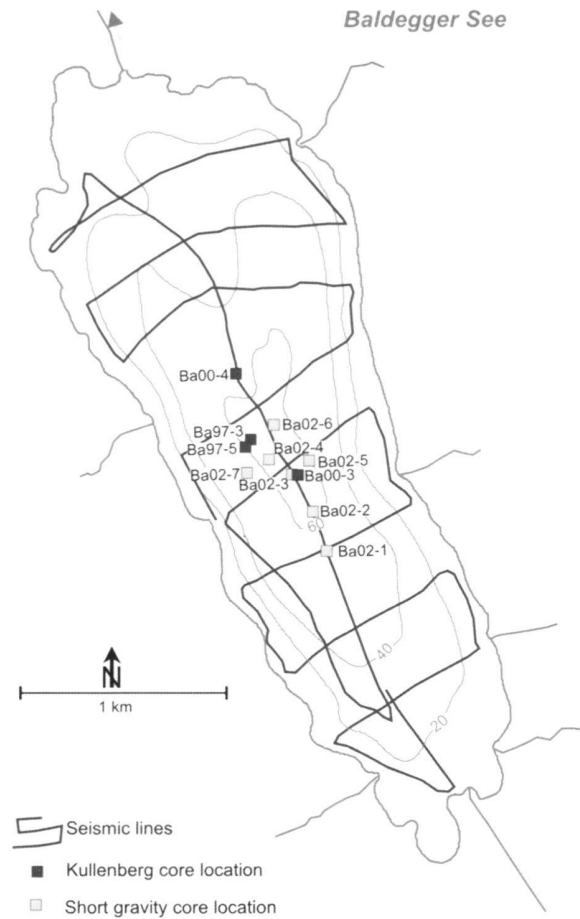


Fig. 7. Bathymetry, seismic survey grid and coring locations of Baldegg See.

top caused by an increased turbidite frequency and a higher water content within the uppermost sediments. The trend is only interrupted by the decreased productivity during the Little Ice Age. A further interval of increased turbidite frequency occurs between 8000 and 10,000 cal y BP.

The core-to-core correlations of Baldegg See are summarized in Figure 9. Seven events can be distinguished comprising mainly small-scale-in-situ deformation structures, which are best seen within the finely laminated varved sequences.

BA1: The youngest event in the sedimentary record of Baldegg See shows several clear in-situ deformation structures (Fig. 9): Within a zone of about 40 cm liquefaction structures within alternations of silts and carbonate-rich mud, disturbed varve lamination and folded layers occur. As also the short cores penetrate through this event horizon deformation structures could be found within 6 of 10 sediment cores indicating the widespread deformation throughout the lake basin. Event BA1 is correlated to the historic Unterwalden earthquake in 1601 AD (Monecke et al. 2004).

BA2: Event BA2 comprises liquefaction structures within an alternation of sandy silts and carbonate mud as well as

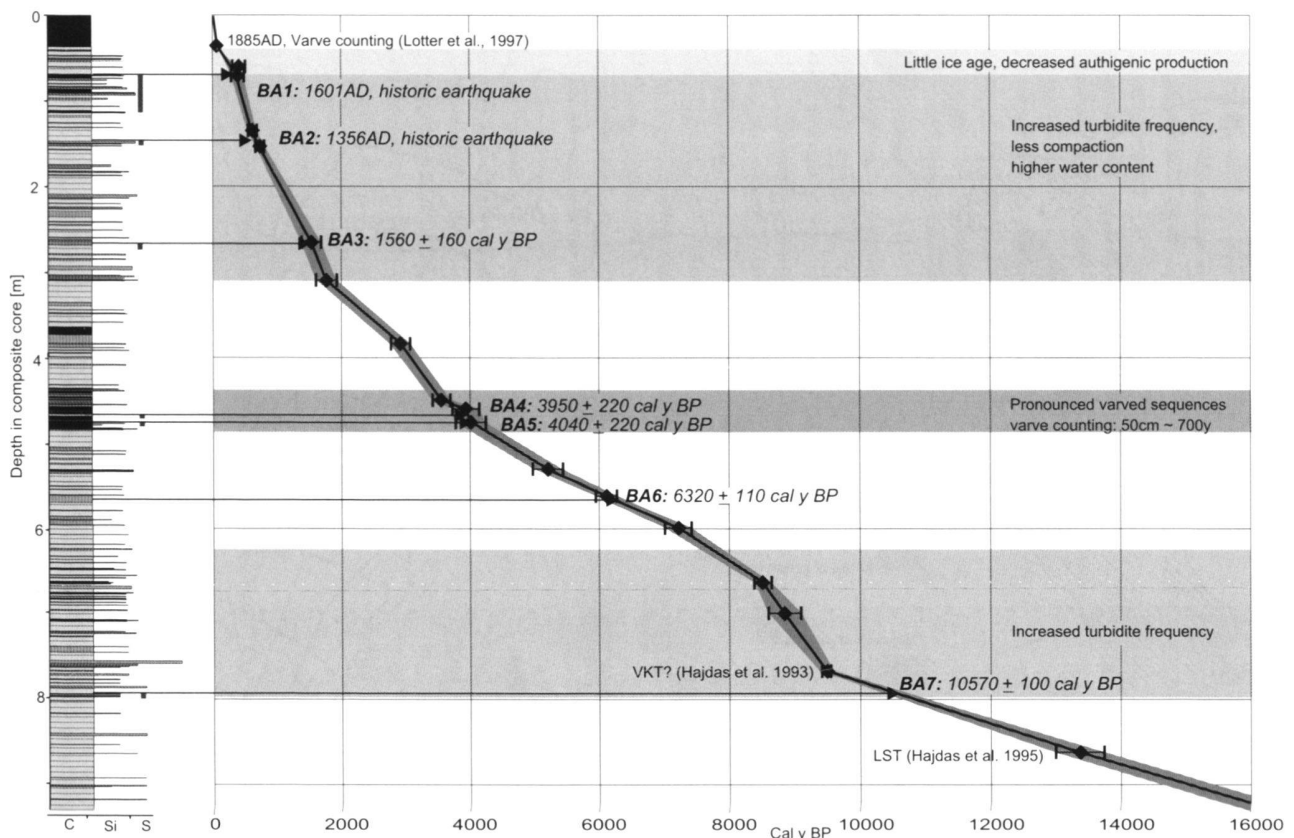


Fig. 8. Composite lithology log and depth/age relationship of sediments in Baldegger See. Radiocarbon ages are mean values of calibrated 2 sigma age ranges (cal y BP, see table 1). Legend as in Fig. 4.

slightly disturbed layering (Fig. 9). Deformation structures are found within 3 of 5 sediment cores. The event horizon is correlated to the 1356 AD Basel earthquake, which affected also the northern part of the study area (Monecke et al. 2004; Mayer-Rosa & Cadot 1979).

BA3, BA4 and BA5: These three events include disturbed lamination and microfaults within 1–7 cm thick intervals of varved sequences (Fig. 9, Fig. 10). Event horizons BA3 and BA4 show clear deformation within one core, whereas in the other cores, varves are missing or not as well preserved, rendering the identification of deformation more difficult. Within event BA5, on the other hand, slight disturbances of the varve lamination are visible in all three cores. The events BA3, BA4 and BA5 have an age of ~1560 cal y BP, ~3950 cal y BP and ~4040 cal y BP, respectively. Events BA4 and BA5 are very similar in age but do not represent only one event, as the relative deformation structures are clearly separated by an interval of undisturbed, finely laminated varves.

BA6: This event represents an uncharacteristic deformation feature in Baldegger See as it comprises a large-scale mass-flow deposit (Fig. 9). It can only be found at the base of sediment core Ba004, whereas the other cores show neither deformation features nor a mass-flow induced turbidite. The

mass-flow deposit is indicated also in the seismic lines and in the bathymetric data of the lake (Fig. 7). Mass-failure took place at ~6320 cal y BP.

Ba7: Within the lowermost sedimentary record recovered in core Ba97-5 the layering of a 2 cm thick sequence of carbonate-rich mud and silty turbidites is disturbed showing slightly folded layers (Fig. 9). This small deformation occurred at ~10,570 cal y BP

Deformation structures in Seelisberg Seeli

Seelisberg Seeli is a small Alpine lake located within the Helvetic nappes at an altitude of 738 m a.s.l. and bounded by a steep cliff at the southern lake side (Fig. 1b). It is possibly formed by combined tectonic and karst processes and has a surface area of only about 0.2 km² but reaches a maximum water depth of 37 m (Fig. 11). One small tributary, that is active only during periods of strong rainfalls, feeds the lake (Theiler et al. 2003). The seismic data shows only poor penetration of the acoustic signal probably due to gas-rich sediments. Four short gravity cores and three long UWITEC cores reaching a maximum sediment depth of 14 m were taken in the central part of the basin. As sediment cores at shallower

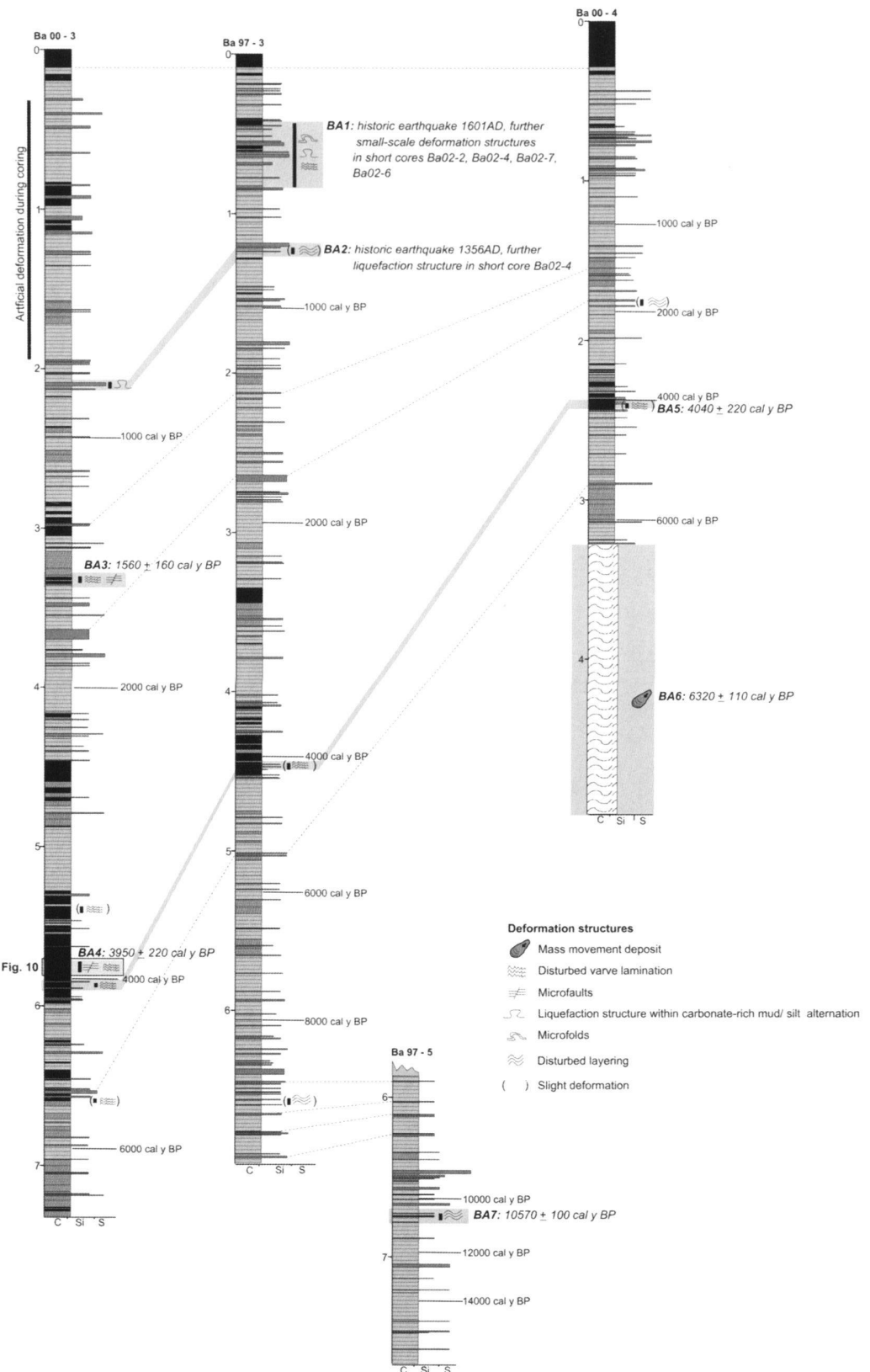


Fig. 9. Core-to-core correlations of events within the sedimentary record of Baldeger See. Lithology legend as in Fig. 4. See Fig. 7 for coring locations.

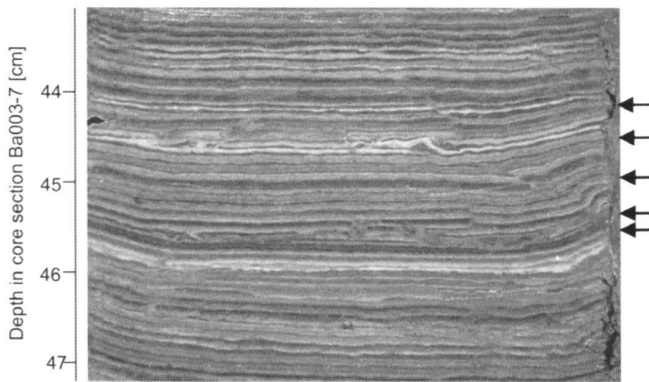


Fig. 10. Disturbed varve lamination in Baldeger See in core section Ba003-7 related to event BA4.

water depth were influenced by bioturbation and/or slope instabilities and show incomplete sedimentary records, only one short core and two long sediment cores taken in the deepest area of the basin were considered for paleoseismic investigations.

The sediments of Seelisberg Seeli represent a mixed sedimentary record of elastically and biochemically dominated processes (Fig. 12, Fig. 13). At the base of the sedimentary record at 14 m depth, gravels of limestones were found, overlain by a ~2 m thick sequence of Late Glacial clays with intercalated sandy turbidites. Towards the top the content of organic matter slowly increases. The regular deposited sediment in the uppermost 7 m to 8 m consist of organic-rich carbonate mud with some larger plant remains similar to gyttja deposits. Locally a well-developed fine lamination of alternating dark organic-rich and white calcite-rich layers is visible. These intervals are interpreted as biochemical varves but they are less well-developed compared to Baldeger See due to abundant plant debris and very thin calcite layers. Remarkable is the large number of a few mm up to 20 cm thick red-colored silty turbidites, which are generated during flood events (Theiler et al. 2003). Thicker gray-colored sandy to silty turbidites are interpreted as mass-flow generated turbidites involving coarser-grained near-shore material. Furthermore, one rockfall deposit and one unit of overthrust lake sediments occur (Fig. 13).

The sedimentary record in Seelisberg Seeli reaches back to about 16,000 cal y BP (Fig. 12). The age model is based on a well-defined radiocarbon chronology showing increasing sedimentation rates from only 2 cm in 100 years below 7000 cal y BP to about 12 cm in 100 years towards the top, due to increased authochthonous production and a low degree of compaction in the uppermost sediments.

Thirteen events, named SEL1 to SEL13, can be determined within the sedimentary record of Seelisberg Seeli comprising large-scale mass movement deposits as well as small-scale in-situ deformation structures (Fig. 13):

SEL1: The youngest event can be seen in two cores in a

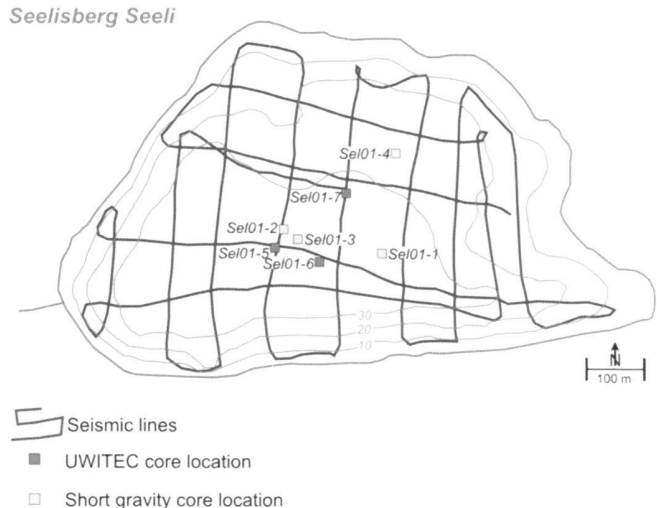


Fig. 11. Bathymetry, seismic survey grid and coring locations in Seelisberg Seeli.

sediment depth of 60 cm comprising a slight liquefaction structure within an alternation of silts and carbonate-rich mud as well as a microfault within finely laminated organic- and carbonate rich mud. These weak deformations can be correlated to the historic 1774AD Altdorf earthquake (Monecke et al. 2004).

SEL2: In a sediment depth of 1–2 m a mass-movement deposit occurs, consisting of a 60 cm thick segment of overturned and displaced lake sediments, overlain by an up to 60 cm thick “homogenite”. Some rock fragments can be found within the overthrust sequence indicating a rockfall probably from the steep southern lakeside. Event SEL2 is correlated to the historic Unterwalden earthquake in 1601AD (Monecke et al. 2004).

SEL3, SEL9, SEL10: These three events are characterized by large-scale, up to 60 cm thick, gray-colored turbidites, probably generated during mass-failure within near-shore lake deposits. The top of the uppermost turbidite (SEL3) shows oscillating grainsize variations typical for a seiche deposit (Chapron, 1999). The underlying sediments of the two lowermost mass flow deposits (SEL9, SEL10) show slightly disturbed bedding produced during deposition of the moving mass. Event horizons SEL3, SEL9 and SEL10 have an age of ~1610 cal y BP, ~6730 cal y BP and ~7720 cal y BP, respectively.

SEL4, SEL8, SEL11: Small-scale slump units indicated by disturbed layering within 10 cm to 20 cm thick intervals mark events SEL4, SEL8 and SEL11. Slump deposits related to event SEL8 are recorded in two cores almost at the same depth, thus probably correlating to the same event. These small-scale mass-movement deposits are ~2680 cal y BP, ~5120 cal y BP and ~9660 cal y BP old.

SEL5, SEL6: Deformation structures relating to events SEL5 and SEL6 comprise disturbed lamination and micro-

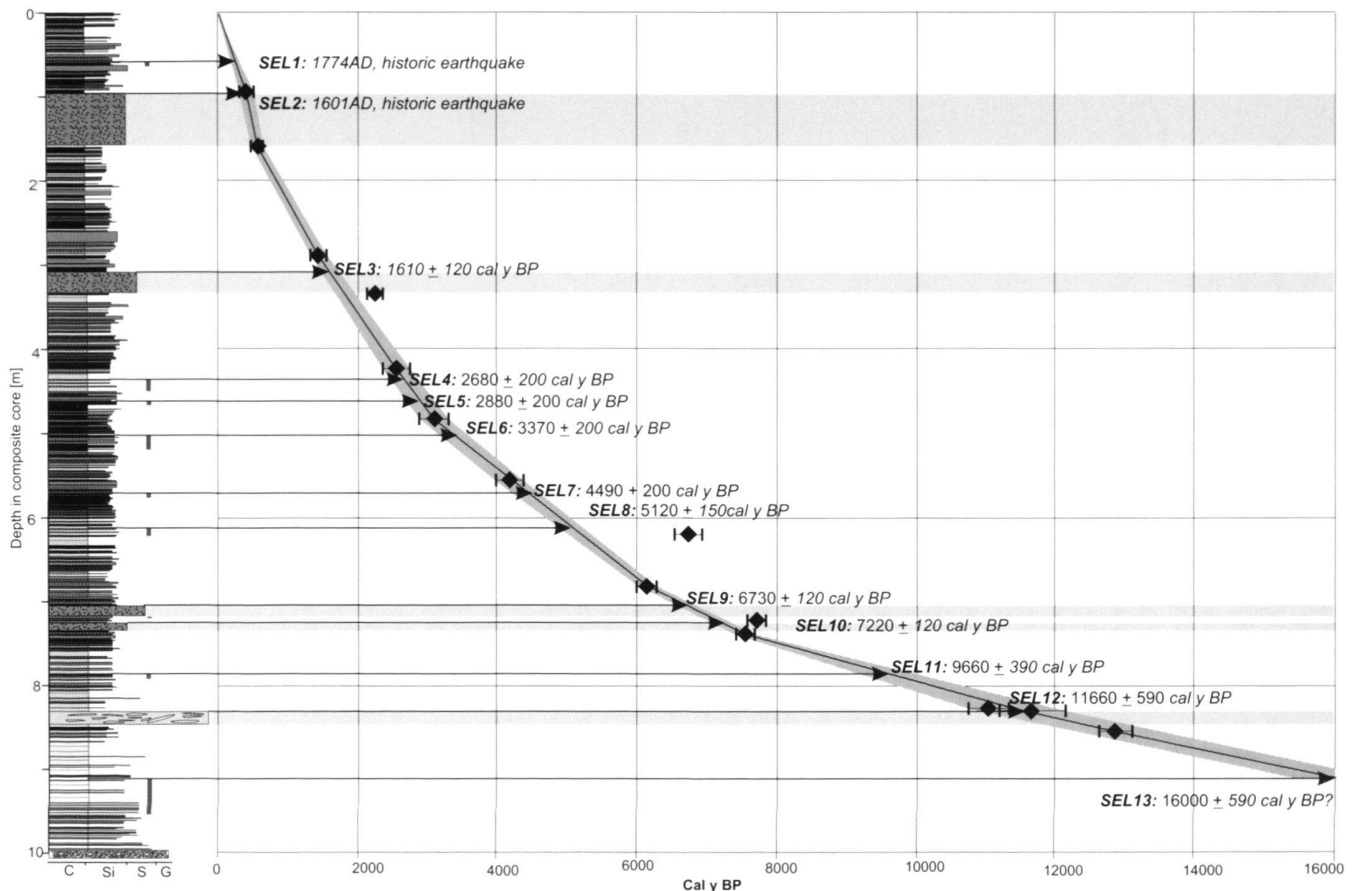


Fig. 12. Composite lithology log and depth/age relationship of sediments from Seelisberg Seeli. Radiocarbon ages are mean values of calibrated 2 sigma age ranges (cal y BP, see table 1). Legend as in Fig. 4.

faults within 5–10 cm thick varved sequences (Fig. 14). They are partly overlain by small- to medium-scale up to 20 cm thick turbidites probably generated during mass-failure. The events SEL5 and SEL6 occurred at ~2880 cal y BP and ~3370 cal y BP, respectively.

SEL7: Microfaults and slight disturbances within an alternation of organic-rich carbonate mud and thin flood-generated turbidites can be observed in two overlapping core sections of sediment core Sel01-5 within a 5 cm thick interval. Deformation occurred at ~4490 cal y BP.

SEL12: Within a 20–50 cm thick interval in the lower sedimentary record coarse, up to 10 cm thick limestone debris occur. They are embedded within largely disturbed layered lake sediments and represent probably a rockfall deposit from the steep southern lakeside dated at ~11,660 cal y BP.

SEL13: Pseudonodules, caused by liquefaction, occur within a 50 cm thick sequence of alternating glacial clays and sandy turbidites in the lowermost sedimentary record. The dating of this event is poorly constrained but deformation must have occurred during early lake sedimentation within a still glacially influenced environment around 16,000 cal y BP.

Events in Vierwaldstätter See (Lake Lucerne)

Paleoseismic investigations in Central Switzerland include a separate study of Vierwaldstätter See carried out by Schnellmann et al. (2002 and 2006, this volume), which is here only summarized. Vierwaldstätter See lies at the border of the Alpine range and is the largest lake in this region with a surface area of 116 km². The lake is divided into seven sub-basins reaching a maximum water depth of 210 m. Four major inflows feed the lake and build up large delta complexes. For paleoseismic investigations the central western basin was chosen, which lacks major deltas and has a low sedimentation rate with faintly laminated mud. More than 300 km of high-resolution seismic lines were obtained imaging large-scale mass-movement deposits that interrupt the regular lake sedimentation (Fig. 15). Based on seismic-stratigraphic correlation, twenty events of mass-failure are determined during the Late Pleistocene/Holocene (Schnellmann et al. 2006). Six of these events including the 1601 AD Unterwalden earthquake are characterized by multiple synchronous mass-failures at different lake sides. Therefore, a seismic trigger mechanism could be as-

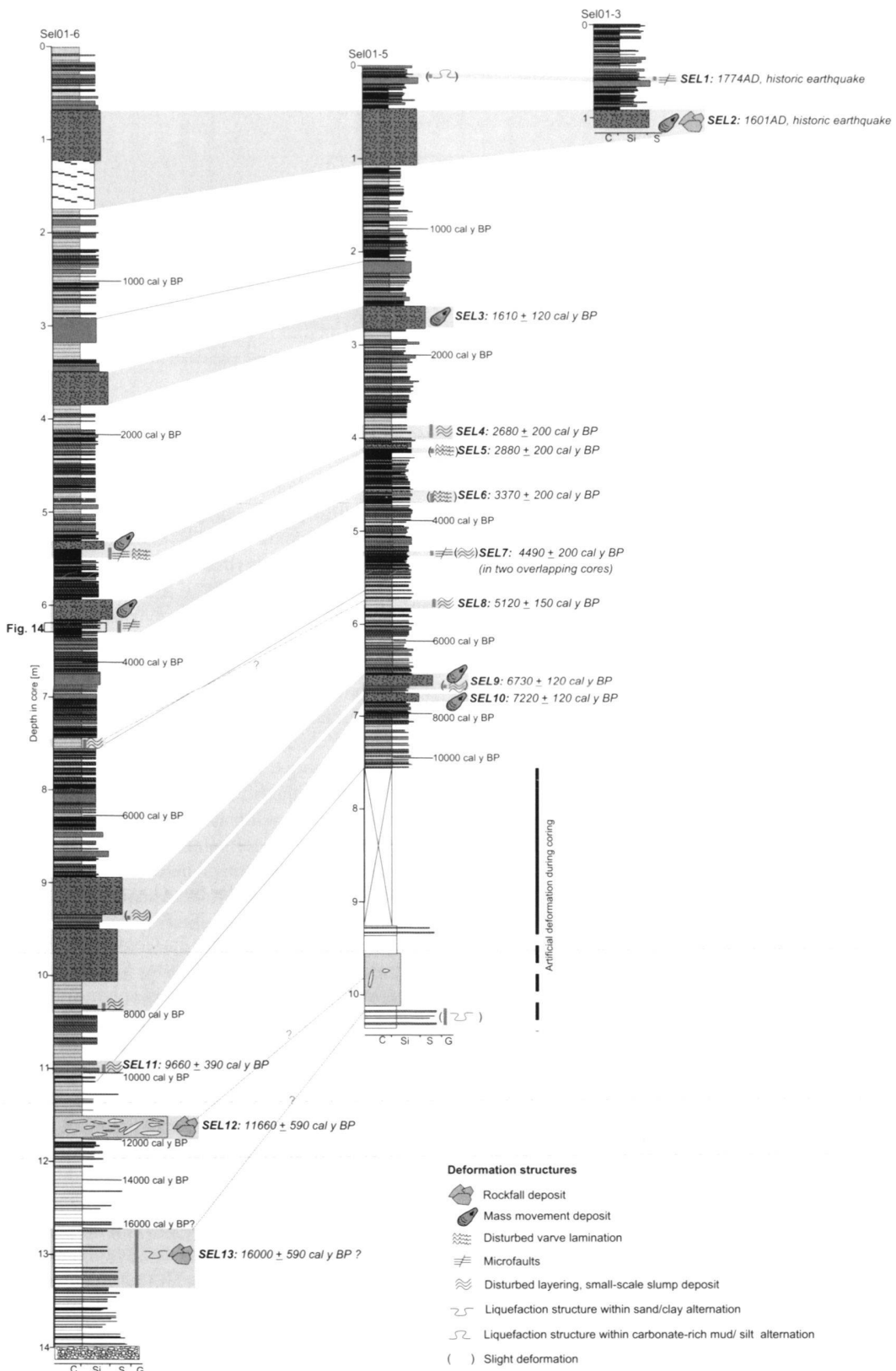


Fig. 13. Core-to-core correlations of events within the sedimentary record of Seelisberg Seeli. Lithology legend as in Fig. 4. See Fig. 11 for coring locations.

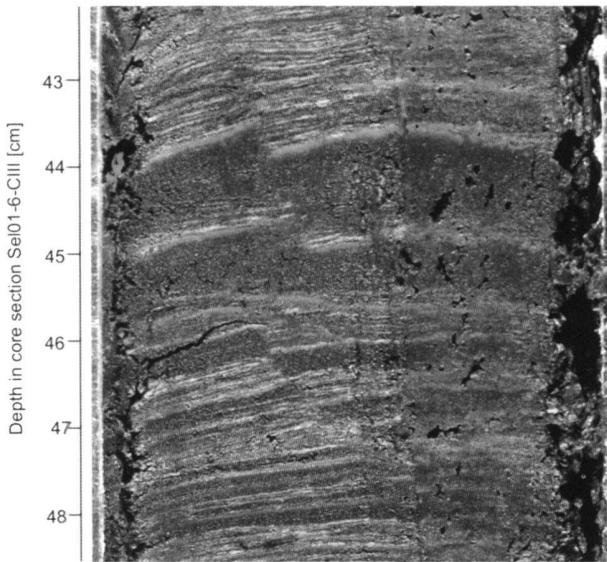


Fig. 14. Microfaults within alternating varves and flood-generated turbidites of Seelisberg Seeli (core section Sel01-6-CIII).

signed (Schnellmann et al. 2002). Long sediment cores reach the different seismic stratigraphic event horizons and allow the dating of the events, compiled in Figure 16.

Determination of earthquakes

The observed deformation structures in lake sediments of Central Switzerland are potentially generated during earthquake shaking. However, other triggering mechanisms have to be considered and the probability of a seismic event has to be evaluated by classifying the deformation structure, the distribution within a single lake and the correlation between different lakes. Small-scale in-situ deformation structures can directly indicate an earthquake trigger mechanism, e.g. if liquefaction structures or deformed varves occur without evidence of sediment overload or disturbances by mass-flow deposition. Ideally the deformation structure can be seen within several cores from one lake to demonstrate the regional impact of seismic shaking and to exclude coring artifacts. Large-scale mass movements, on the other hand, can be generated spontaneously at the lake sides especially within mountain areas and highly dynamic sedimentary systems. Therefore, only multiple synchronous mass-failures at different lake sides are highly indicative for a regional seismic trigger mechanism. Figure 16 summarizes the observed deformation structures in the different lake sediments in Central Switzerland using a three-level scale for in-situ deformation features and a two-level scale for mass movement deposits, thus assigning a probability of earthquake origin to the single events within one lake (data of Vierwaldstätter See after Schnellmann et al. 2006). As a second step events between different lakes are correlated, as the synchronism and widespread regional dis-

tribution of deformation structures is a strong argument for a seismic trigger mechanism.

Combining the local and regional evidence of deformation features, prehistoric earthquakes can be determined with a confidence level ranging from high to low: 1) A high probability of earthquake triggering is assigned to events, which show clear evidence of earthquake-induced deformation at least in one lake, like e.g. multiple synchronous mass failure or clear in-situ deformation structures in several sediment cores. A high probability is also assigned, when synchronous deformation structures are observed in three or more lakes. 2) A medium probability of a seismic trigger is proposed for events showing a medium evidence of earthquake induced deformation in one lake (clear in-situ deformation at least within one core) coinciding with deformation within at least one more lake with coincidence in timing. 3) A low probability is assigned to events, which are visible only within one lake showing a medium evidence of earthquake induced deformation, which means clear in-situ deformation structure within one sediment core.

It has to be considered that quality and quantity of data decreases with increasing age of the sedimentary record. Within the uppermost sediments down to approximately 500 cal y BP a dense, excellent database exists due to numerous short cores, previous investigations that concentrated on the youngest sediments (e.g. Lotter et al. 1997a in Baldegger See; Siegenthaler & Sturm 1991 and Siegenthaler et al. 1987 in Vierwaldstätter See) and a very precise dating due to the availability of historic data. For the period prior to 3000 cal y BP, only three lakes can be compiled because of the short sedimentary record of Lungerer See. The sedimentary records of Baldegger See, Seelisberg Seeli and Vierwaldstätter See are less constrained in the lowermost sediments, as only few cores reach the oldest sediments. Furthermore, radiocarbon ages are difficult to obtain within still glacially influenced sediments of the Late Pleistocene and calibrated radiocarbon ages have quite large uncertainty ranges.

As the northern study area can be influenced by large earthquakes in the Basel region (Mayer-Rosa & Cadiot 1979), we include also paleoseismic data from on-fault surface mapping and lake deposits in the Basel area (Becker et al. 2002, 2005; Ferry et al. 2005). In this region a five-stage scale of probability of earthquake-triggering ranging from very high to very low is proposed for the different events. In Fig. 16 we include only the three highest levels of probability closely related to our probability scale.

Historic earthquakes and calibration of earthquake-induced deformation

Traces of three large historic earthquakes have been found in the sedimentary record of the four investigated lakes in Central Switzerland (Fig. 16, Fig. 17) (Monecke et al. 2004; Schnellmann et al. 2002; Siegenthaler & Sturm 1991): The clearest and most widespread deformation occurred during the $M_w = 6.2$

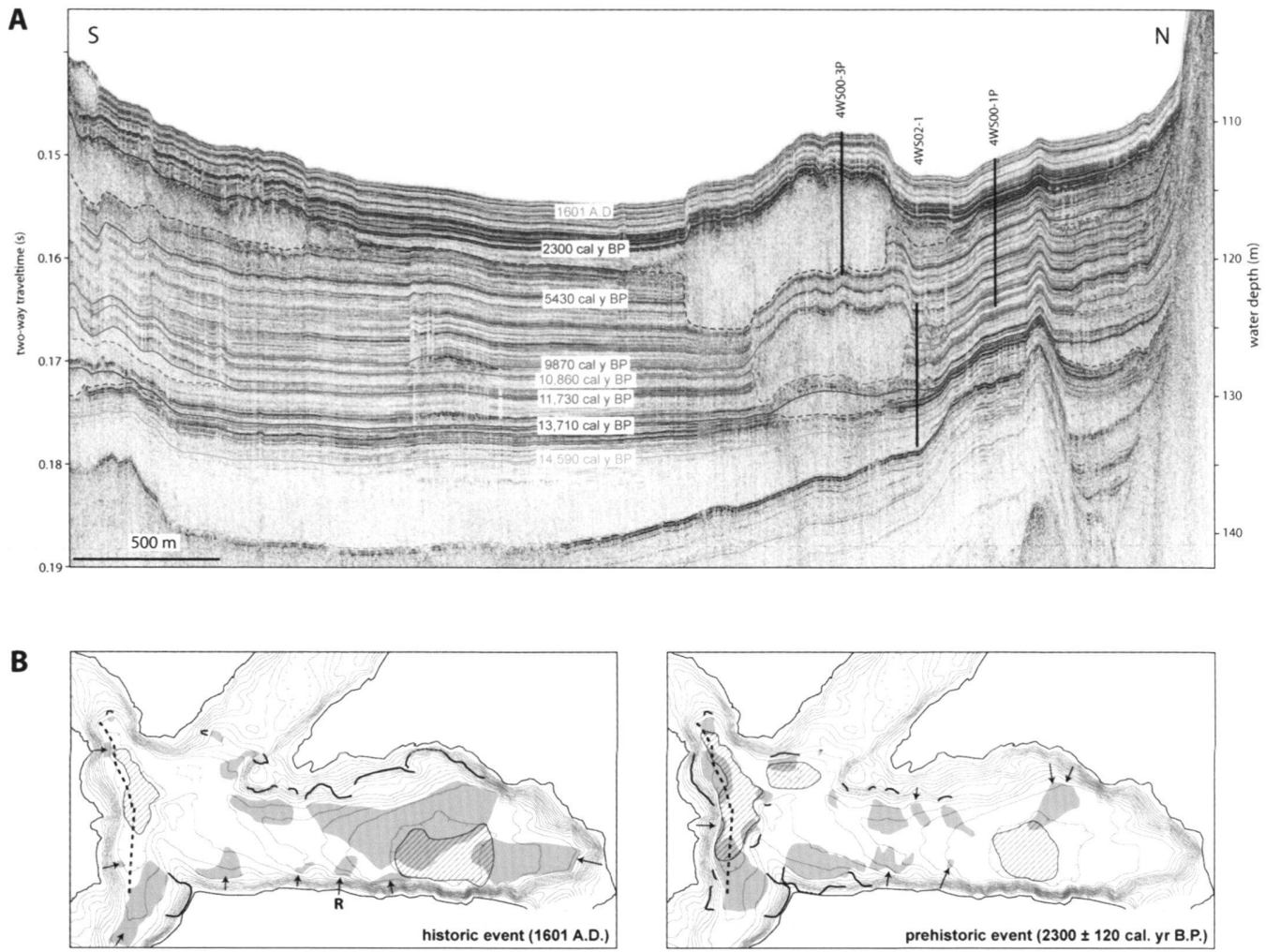


Fig. 15. Multiple mass-flow deposits in Lake Lucerne. (A) 3.5 kHz seismic profile showing the subsurface of Chrüztrichter basin. Colored solid lines mark seismic stratigraphic horizons allocated to the top of specific mass-flow deposits and megaturbidites. The base of these deposits is marked with dashed lines. Note that some of the seismic stratigraphic horizons coincide with the top of more than one mass-flow deposit and thus indicate synchronous deposition. See dashed bold line in Figure 15B for location of the profile. (B) The left and right panels show multiple mass-flow horizons relating to the historic 1601AD earthquake and to a prehistoric event, respectively. Equidistance of the bathymetric lines is 10 m. Dotted lines contour 5 m intervals and aim to clarify the basin geometry. Grey shadings indicate mass-flow deposits and hatched surfaces mark megaturbidites. Mass-flow deposits, which evolved from subaerial rockfalls are denoted with 'R'. Bold black lines depict failure scars.

Unterwalden earthquake in 1601 AD with the epicenter in the middle of the study area causing clear in-situ deformation structures in Baldegger See and large-scale mass-failures in Vierwaldstätter See, Lungerer See and Seelisberg Seeli. The $M_w = 5.9$ event in Altdorf in 1774 AD affected only the Eastern part of the study area and caused slight deformation in Seelisberg Seeli and mass-failure in the Eastern lake basin of Vierwaldstätter See. The most recent 1964 AD Alpnach earthquake with a magnitude of 5.7 apparently did not affect the investigated lake sediments not even within the nearby Sarner See. Traces of the devastating $M_w = 6.9$ event in Basel in 1356 AD, however, could be found in northernmost Baldegger See, only.

The signature of the historic earthquakes can be used to calibrate earthquake-induced deformation in lake sediments in Central Switzerland. Although the type and extent of deformation during seismic shocks depend on numerous factors like sediment type, geometry of the lake basin and amplification of shaking due to site effects, deformation of lake sediments becomes common and widespread only if the lakes are situated within or close to the isoseismal line of intensity VII (Fig. 17, Monecke et al. 2004; Sims 1973 and 1975; Hibsch et al. 1997). Furthermore, a minimum earthquake size of $M_w = 5$ to $M_w = 5.5$ is required as a certain duration and amplitude of shaking is necessary to deform the lake sediments and to pro-

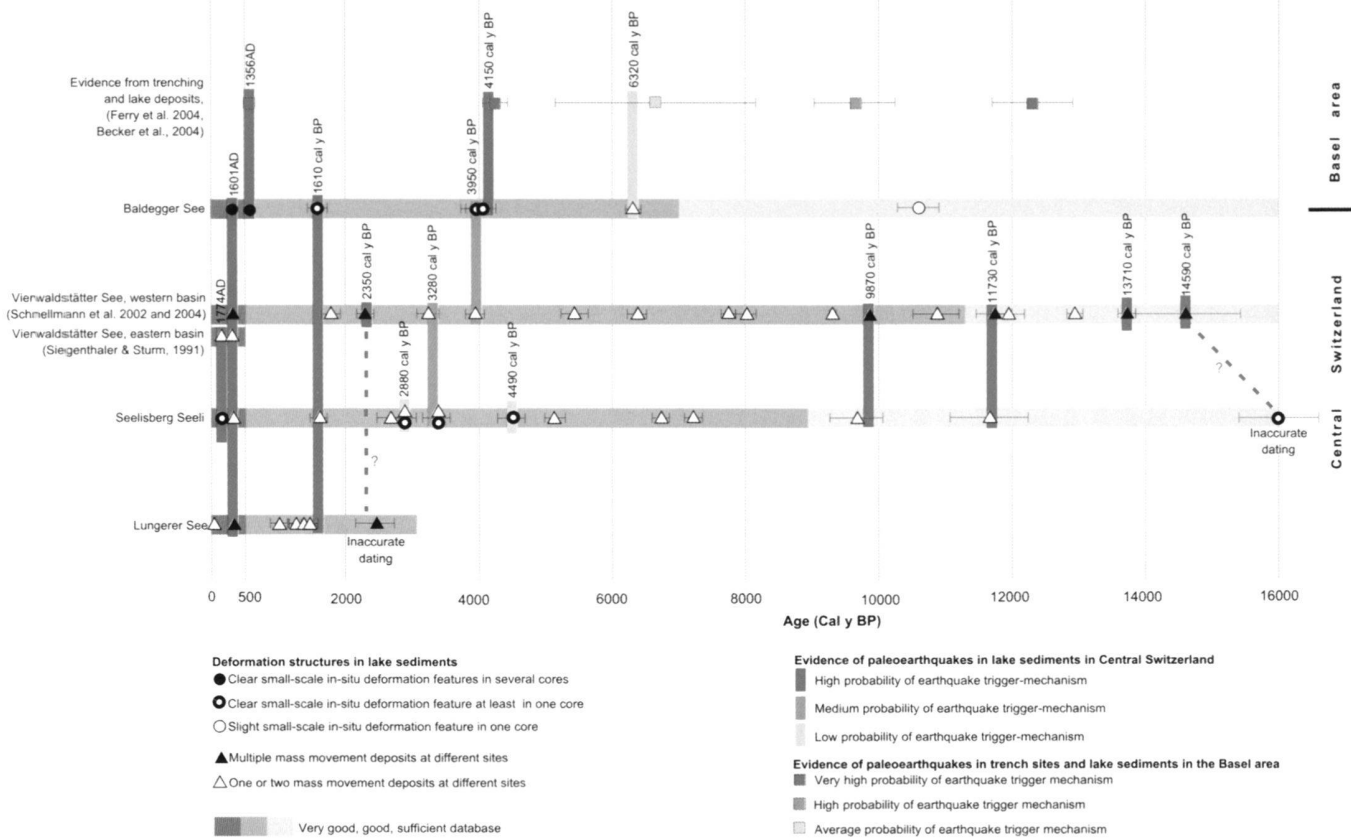


Fig. 16. Correlation of deformation structures in Vierwaldstätter See (after Schnellmann et al. 2006), Lungerer See, Baldegger See, Seelisberg Seeli and determination of historic and prehistoric earthquakes in Central Switzerland. Paleoseismic events with a high probability of a seismic trigger mechanism show clear evidence of earthquake-induced deformation at least within one lake or deformation structures within three or more lakes. Events with medium probability show a medium evidence of earthquake-induced deformation in one lake and further deformation in another lake. Events with low probability are visible only within one lake and show a medium evidence of earthquake-induced deformation. Deformation structures in Baldegger See partly correlate with paleoseismic events in the Basel area proposed by Ferry et al. 2004 and Becker et al. 2002.

duce e.g. liquefaction structures (Obermeier 1996; Moretti et al. 1999). Within this study the threshold might be even higher as indicated by the lack of sediment deformation in Sarner See during the $M_w > 5.7$ Alpnach earthquake in 1964 AD.

The spatial distribution of deformation throughout the different lake basins can be used to determine the size and epicenter of the prehistoric events. Epicenters of historic earthquakes are concentrated around Sarnen and Altdorf in Central Switzerland and around Basel in Northern Switzerland (Fig. 1; Deichmann et al. 2000; Fäh et al. 2003). Assuming that also prehistoric earthquakes were generated within these three regions the following assumptions can be made (Fig. 17): Large earthquakes in the Basel area with magnitudes similar to the $M_w = 6.9$ earthquake in 1356 AD would affect only Baldegger See in the northern part of the study area. On-fault mapping of surface deformations in the Basel region revealed no events with $M_w > 6.9$ (Ferry et al. 2005), consequently, Vierwaldstätter See, Seelisberg Seeli and Lungerer See are not influenced by Basel earthquakes. A larger earthquake in the southwestern

part of Central Switzerland with epicenter and size similar to the $M_w = 6.2$ Unterwalden earthquake in 1601 AD would affect all investigated lakes. Less strong earthquakes will not be recorded in Baldegger See and subsequently not in Lungerer See and Seelisberg Seeli. Medium to large earthquakes in the Altdorf region do only affect Seelisberg Seeli and the Eastern part of Vierwaldstätter See, implying that a hypothetical $M_w = 6.2$ event in the Altdorf region is probably not recorded within the other lake basins (see dashed line in Fig. 17).

Prehistoric earthquakes

Basel region:

As indicated by the historic 1356 AD Basel earthquake, strong seismic shocks in the Basel region can cause deformation within the sediments of Baldegger See. The deformed varves within event BA5 at 4040 cal y BP correlate with a highly probable seismic event recorded in the trench sites (Ferry et al. 2005,

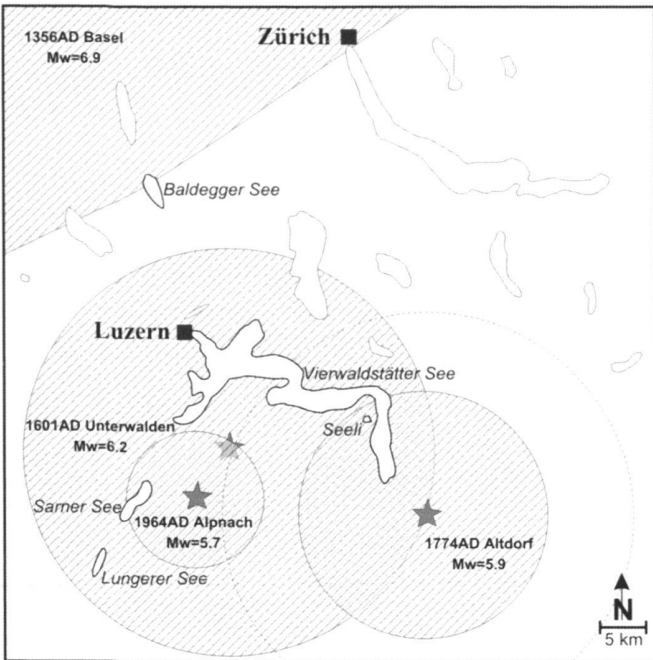


Fig. 17. Areas with expected groundshaking of intensity \geq VII of the four largest historic earthquakes affecting the area of Central Switzerland during the last 1000 years. Dashed line mark area with expected groundshaking of intensity VII of hypothetical $M_w = 6.2$ event in the Altdorf region (intensity attenuation relation for 1964 Alpnach, 1774 Altdorf and 1601 Unterwalden earthquakes after Swiss Seismological survey, 2002; 1356 Basel earthquake after Mayer-Rosa & Cadot, 1979).

Becker et al. 2005). Furthermore, the large-scale slump deposit at 6320 cal y BP (BA6) could be related to an event with only a low probability of seismic shaking. Further events recorded in the trench sites and lake deposits in the Basel region could not be detected in the sedimentary record of Baldegg See.

Central Switzerland:

1) High probability: With high probability six large prehistoric earthquakes can be assumed in Central Switzerland during the last 15,000 years (Fig. 16). Five of these events are marked by multiple synchronous mass-failures in the western basin of Vierwaldstätter See (Schnellmann et al. 2002 and 2006) and correlate with deformation structures in Seelisberg Seeli and Lüniger See: The event at 2350 cal y BP generated might correlate with multiple mass-failure in Lüniger See (LNG7). However, the dating in this part of the record is uncertain. The events at 9870 cal y BP and 11730 cal y BP are marked by a small-scale slump and a rockfall in Seelisberg Seeli (SEL11, SEL12). No further deformations are recorded during the event at 13,710 cal y BP. The oldest event at 14,590 cal y BP probably correlates with a clear liquefaction structure in Seelisberg Seeli (SEL13). Remarkable is that none of these events could be found in the sedimentary record of Baldegg See.

The youngest event at 1610 cal y BP is recorded by deformed varves in Baldegg See (BA3), and large-scale mass failures in Lüniger See (LNG6) and Seelisberg Seeli (SEL3) with a good coincidence in timing. Despite the occurrence of only a single mass movement deposit in the two latter lakes, these are of extraordinary size within the sedimentary record of Lüniger See and Seelisberg Seeli (Fig. 4; Fig. 13). The seismic data of Vierwaldstätter See show only one small-scale mass movement deposit (Schnellmann et al. 2006). However, several turbidites can be found in the sediment cores within the same stratigraphic level, which could have been generated during small-scale mass movements, which are beyond the resolution of the seismic data. They could also represent reworked material from on-shore coseismic landslides (ibson, 1996). It is possible that the impact on Vierwaldstätter See was low because a lot of instable sediment at the slopes was already mobilized during the previous earthquake at 2350 cal y BP.

The deformation pattern of these six prehistoric events with a high probability matches well with the historic 1601 AD Unterwalden earthquake with $M_w = 6.2$, as two or more lakes within the study area are affected and/or the western basin of Vierwaldstätter See shows widespread multiple mass-failures. Therefore, we assume that epicenter and size of these prehistoric events were similar. The lack of deformation at Baldegg See during most of these events could indicate an epicenter located more towards the South or slightly less strong ground shaking.

2) Medium probability: Medium probability of a seismic trigger mechanism is assigned to two events in Central Switzerland at 3280 cal y BP and 3950 cal y BP. The younger event comprises deformed lamination and microfaults within varved sequences and a medium-scale mass-flow deposit in Seelisberg Seeli (SEL 6). Furthermore, a single large-scale mass movement deposit in the eastern part of the western sub-basin of Vierwaldstätter See occurs (Schnellmann et al. 2006). As these deformations are concentrated in the eastern part of the study area it is possible that the epicenter of this potential event lies within the Altdorf region with a size comparable to the 1601AD Unterwalden earthquake.

As no earthquake-induced deformation was observed in the trench sites in the Basel region the deformed varves in Baldegg See at 3950 cal y BP correlate possibly with a small-scale mass movement deposit in Vierwaldstätter See. As a large earthquake around Sarnen would have been recorded also in the other lakes the epicenter of this potential event lies possibly further to the North closer to Luzern and Baldegg See.

3) Low probability: Two events in the sedimentary record of Seelisberg Seeli (SEL5, SEL7) show deformed finely laminated sediments. However, as they are only recorded within one lake the probability of a seismic trigger mechanism is set low. The deformations in Seelisberg Seeli occurring at 2880 cal y BP and 4490 cal y BP could have been generated during seismic shocks in the Altdorf region of at least the size of the $M_w = 5.9$ Altdorf event in 1774 AD.

Conclusions

The present study shows that historic and prehistoric earthquakes are recorded in the sedimentary archives of recent lake deposits. Earthquake-induced deformation structures comprise large-scale mass movement deposits and small-scale in-situ deformation features depending on lake basin geometry, dominant sedimentary processes within the lake, and local groundshaking. In order to obtain a paleoseismic record for Central Switzerland and to determine the size and epicenter of paleoearthquakes, four lakes in Central Switzerland distributed within an area of approximately 2000 km² were investigated. Traces of three large historic earthquakes were examined, allowing the calibration of earthquake-induced deformation: A minimum earthquake size of about $M_w = 5.7$ and local ground shaking of intensity VII is required to produce clear and widespread deformation within the lake deposits. An earthquake of $\sim M_w = 6.2$ with the epicenter in the middle of the study area would be recorded in all investigated lakes. Seismic events with smaller magnitudes or different epicenters may be recorded only within one lake.

A highly probable prehistoric event in the Basel region (Ferry et al. 2005) is also evident in Baldeger See deposits. Furthermore, with a high probability at least six larger earthquakes with epicenter and size similar to the 1601 AD Unterwalden earthquake occurred in Central Switzerland in prehistoric times during the last 15,000 cal y BP. Traces of further prehistoric earthquakes are less well-constrained but might indicate one event closer to Lucerne and three events in the Alt-dorf region with magnitudes of at least $M_w = 5.9$.

The paleoseismic data shows irregular recurrence intervals of large earthquakes in Central Switzerland varying between ~ 200 years and ~ 5000 years with a clustering of earthquakes during the Late Pleistocene/Early Holocene and since about 4000 cal y BP. Earthquake activity mainly reflects the ongoing collision of the Alpine belt as it has been described by Persaud & Pfiffner (2004) for the eastern Swiss Alps. Potentially, the higher frequency in the oldest paleoseismic record images also the isostatic rebound after the retreat of the glaciers in the Alpine valleys as reported for Northern Europe (Ringrose 1987; Mörner 2000). The clustering during the last 4000 y BP can partly be an effect of the increasing quality of the database but probably reflects a periodic activation of a seismogenic zone in Central Switzerland during more recent times.

Acknowledgements

We thank Adi Gilli and Amik Theiler for their help during field and laboratory work; Robert Hofmann, Urs Gerber, Alois Zwysig and Richard Niederreiter for technical support. We would like to give special acknowledgement to Jürg Beer and Bernd Zolitschka for their helpful and comprehensive comments on an earlier version of the manuscript. This study is part of the Paleoseis Project that is funded by the Swiss National Funds (SNF) and the Swiss Commission for the Safety of Nuclear Installations (HSK).

REFERENCES

ALLEN, J. R. L. 1982. Sedimentary structures, vol. II. Developments in Sedimentology, vol. 30B. Elsevier, Amsterdam (663pp).

ANKETELL, J. M., CEGLA, J. & DZULYNSKI, S. 1970. On the deformational structures in systems with reversed density gradients. *Ann. Geol. Soc. Pol.* XL, 3–30.

BECKER, A., DAVENPORT, C. A. & GIARDINI, D. 2002. Paleoseismicity studies on end-Pleistocene and Holocene lake deposits around Basle, Switzerland. *Geophys. J. Int.* 149, 659–678.

BECKER, A., FERRY, M., MONECKE, K., SCHNELLMANN, M. & GIARDINI, D. 2005: Multiarchive paleoseismic record of late Pleistocene and Holocene strong earthquakes in Switzerland. *Tectonophysics* 400, 153–177.

BRONK RAMSEY, C. 1995. Radiocarbon calibration and analysis of stratigraphy: The OxCal Program. *Radiocarbon* 37(2), 425–430.

BRONK RAMSEY, C. 2001. Development of the radiocarbon program OxCal. *Radiocarbon* 43 (2A), 355–363.

CHAPRON, E., BECK, C., POURCHET, M. & DECONINCK, J. F. 1999. 1822 earthquake triggered homogenite in Lake Le Bourget (NW Alps). *Terra Nova* 11, 86–92.

DAVENPORT, C. 1994. Geotechnical consequences of ground motion: hazard perspectives. *Geologie en Mijnbouw* 73, 339–356.

DEICHMANN, N., BALLARIN DOLFIN, D. & KASTRUP, U. 2000. Seismizität in der Nord- und Zentralschweiz. Nagra, Technischer Bericht, 93pp.

DOIG, R. 1986. A method for determining the frequency of large-magnitude earthquakes using lake sediments. *Can. J. Earth Sci.* 23, 930–937.

FAH, D., GIARDINI, D., BAY, F., BERNARDI, F., BRAUNMILLER, J., DEICHMANN, N., FURRER, M., GANTNER, L., GISLER, M., ISENEGGER, D., JIMINEZ, M.J., KÄSTLI, P., KOGLIN, R., MASIARDI, V., RUTZ, M., SCHEIDECKER, C., SCHIBLER, R., SCHORLEMMER, D., SCHWARZ-ZANETTI, G., STEIMEN, S., SELLAMI, S., WIEMER, S. & WÖSSNER J. 2003. Earthquake Catalogue of Switzerland (ECOS) and the related Macroseismic Database. *Elogiae Geol. Helv.* 96 (2), 219–236.

FERRY, M., MEGHRAOUI, M., DELOUIS, B. & GIARDINI, D. 2005. Evidence for Holocene paleoseismicity along the Basel-Reinach Active Normal Fault (Switzerland): A seismic source for the 1356 Earthquake in the Upper Rhine Graben. *Geophys. J. I.* 160, 554–572.

GALLI, P. & FERELLI, L. 1995. A methodological approach for historical liquefaction research. In: SERVA, L. & SLEMMONS, D. B. (Eds.), *Perspectives in Paleoseismology*. Ass. of Engineering Geologists, Spec. Publ. 6, 35–48.

HAJDAS, I., IVY, S. D., BEER, J., BONANI, B., IMBODEN, D., LOTTER, A. F., STURM, M. & SUTER, M. 1993. AMS radiocarbon dating and varve chronology of Lake Soppensee: 6000 to 12,000 ^{14}C years BP. *Climate dynamics* 9, 107–116.

HAJDAS, I., IVY OCHS, S. D., BONANI, B., LOTTER, A. F., ZOLITSCHKA, B. & SCHLÜCHTER, C. 1995. Radiocarbon Age of the Laacher See Tephra: $11,230 \pm 40$ BP. *Radiocarbon* 37, 149–154.

HIBSCH, C., ALVARADO, A., YEPES, H., PEREZ, V. H. & SÉBRIER M. 1997. Holocene liquefaction and soft-sediment deformation in Quito (Ecuador): A paleoseismic history recorded in lacustrine sediments. *J. Geodynamics* 24, 259–280.

JIBSON, R. W. 1996. Use of landslides for paleoseismic analysis. *Eng. Geol.* 43, 291–323.

KELTS, K., BRIEGEL, U., GHILARDI, K. & HSÜ, K.J. 1986. The limnogeology-ETH coring system. *Schweiz. Z. Hydrol.* 48, 104–115.

LOTTER, A. F., STURM, M., TERRANES, J. L. & WEHRLI, B. 1997a. Varve formation since 1885 and high resolution varve analysis in hypertrophic Baldegersee (Switzerland). *Aquatic Sciences* 59, 304–325.

LOTTER, A. F., MERKT, J. & STURM, M. 1997b. Differential compaction versus coring artifacts: a comparison of two widely used piston-coring methods. *J. Paleolimnology*, 18, 75–85.

MARCO, S., STEIN, M. & AGNON A. 1996. Long term earthquake clustering: A 50 000-year paleoseismic record in the Dead Sea Graben. *J. Geophysical Res.* 101, 6179–6191.

MAYER-ROSA, D. & CADIOT, B. 1979. A review of the 1356 Basel earthquake. *Tectonophysics* 53, 325–333.

MCCALPIN, J. 1996. *Paleoseismology*. Academic Press, San Diego, 588p.

MING, H. 1991. Bürglen – Kaiserstuhl von Damals bis Heute. Küchler-Verlag, Giswil.

MIGOWSKI, C., AGNON, A., BOOKMAN, R., NEGENDANK, J. F. W. & STEIN, M. 2004. Recurrence pattern of Holocene earthquakes along the Dead Sea transform revealed by varve-counting and radiocarbon dating of lacustrine sediments. *Earth and Planetary Science Letters*, 222, 301–314.

MÖRNER, N. A., TROFTEN, P. E., SJÖBERG, R., GRANT, D., DAWSON, S., BRONGE, C., KVAMSDAL, O. & SIDEN, A. 2000. Deglacial paleoseismicity in Sweden: the 9663 BP Iggesund event. *Quat. Sci. Rev.* 19, 1461–1468.

MONECKE, K., ANSELMETTI, F., BECKER, A., STURM, M. & GIARDINI, D. 2004. Signature of historic earthquakes in lake sediments in Central Switzerland. *Tectonophysics*, 394, 21–40.

MONECKE, K. 2004. Earthquake-induced deformation structures in lake deposits – A Late Pleistocene to Holocene paleoseismic record for Central Switzerland. Unpubl. thesis, ETH Zürich, 154pp.

MORETTI, M., ALFARO, P., CASELLES, O. & CANAS, J. A. 1999. Modelling seismites with a digital shaking table. *Tectonophysics* 304, 369–383.

ÖBERMEIER, S. F. 1996. Use of liquefaction-induced features for paleoseismic analysis – An overview of how seismic liquefaction features can be distinguished from other features and how their regional distribution and properties of source sediment can be used to infer the location and strength of Holocene paleo-earthquakes. *Eng. Geol.* 44, 1–76.

PERSAUD, M. & PFIFFNER, O. A. 2004. Active deformation in the eastern Swiss Alps: post-glacial faults, seismicity and surface uplift. *Tectonophysics* 385, 59–84.

RICCI LUCCHI, F. 1995. Sedimentological indicators of paleoseismicity. In: Serva, L., Slemmons, D. B. (Eds.), *Perspectives in Paleoseismology*. Ass. of Engineering Geologists, Spec. Publ. 6, 7–17.

RINGROSE, P. S. 1989. Paleoseismic (?) liquefaction event in late Quaternary lake sediment at Glen Roy, Scotland. *TerraNova* 1, 57–62.

RODRIGUEZ PASCUA, M. A., CALVO, J. P., DE VICENTE, G., GOMEZ-GRAS, D., 2000. Soft-sediment deformation structures interpreted as seismites in lacustrine sediments of the Prebetic Zone, SE Spain, and their potential use as indicators of earthquake magnitudes during the late Miocene. *Sed. Geol.* 135, 117–135.

SCHNELLMANN, M., ANSELMETTI, F. S., GIARDINI, D., MCKENZIE, J. A. & WARD, S. N., 2002. Prehistoric earthquake history revealed by lacustrine slump deposits. *Geology* 30/12, 1131–1134.

SCHNELLMANN, M., ANSELMETTI, F. S., GIARDINI, D. & MCKENZIE, J. A. 2005. Mass movement-induced fold-and-thrust belt structures in unconsolidated sediments in Lake Lucerne (Switzerland). *Sedimentology*, 52, 271–289.

SCHNELLMANN, M., ANSELMETTI, F. S., GIARDINI, D. & MCKENZIE, J. A. (2006). 15,000 years of mass-movement history in Lake Lucerne: Implications for seismic and tsunami hazard. *Eclog. Geol. Helv.* 99, DOI 10.1007/s00015-006-1196-7.

SEILACHER, A. 1969. Fault-graded beds interpreted as seismites. *Sedimentology* 13, 155–159.

SHILTS, W. W. & CLAGUE, J. J. 1992. Documentation of earthquake-induced disturbance of lake sediments using subbottom acoustic profiling. *Can. J. Earth Sci.* 29, 1018–1042.

SIEGENTHALER, C., FINGER, W., KELTS, K. & WANG, S. 1987. Earthquake and seiche deposits in Lake Lucerne, Switzerland. *Eclogae Geol. Helv.* 80, 241–260.

SIEGENTHALER, C. & STURM, M. 1991. Die Häufigkeit von Ablagerungen extremer Reuss- Hochwasser. Die Sedimentationsgeschichte im Urnersee seit dem Mittelalter. *Mitt. Bundesamt f. Wasserwirtschaft* 4, 127–139.

SIMS J. D. 1973. Earthquake-induced structures in sediments of Van Norman Lake, San Fernando, California. *Science* 182, 161–163.

SIMS J. D. 1975. Determining earthquake recurrence intervals from deformational structures in young lacustrine sediments. *Tectonophysics* 29, 141–152.

STUIVER, M., REIMER, P. J., BARD, E., BECK, J. W., BURR, G. S., HUGHEN, K. A., KROMER, B., McCORMAC, F. G., v.D. PFLICHT, J. & SPURK, M. 1998. INTCAL98 radiocarbon age calibration, 24,000-0 cal BP. *Radiocarbon* 40, 1041–1083.

STURM, M., SIEGENTHALER C. & PICKRILL, R. A. 1995: Turbidites and “homogenites” – A conceptual model of flood and slide deposits. 16th IAS Meeting Abstr. Vol., 170–171.

Swiss Seismological Service 2002. ECOS – Earthquake Catalog of Switzerland. ECOS Report to PEGASOS, Version 31. 3. 2002. SED, Zürich.

THEILER, A., MONECKE, K. & ANSELMETTI, F. 2003. Frequency of strong rainfall events during the Holocene recorded in lake sediments from Seelisberger Seeli in central Switzerland. 3rd Int. Limnogeology Congress Abstr. Vol., 294.

Manuscript received September 24, 2004

Revision accepted July 21, 2006

Published Online First January 12, 2007